This manuscript is a pre-print. It has undergone peer review and has been accepted in the Geological Society of London Special Publications proceedings of the EGC1 but has not yet undergone journal typesetting.

Subsurface storage capacity in structural traps in underexplored sedimentary basins: Hydrogen (H_2) and carbon dioxide (CO_2) storage on the Irish Atlantic margin

Conor M. O'Sullivan[1,2,3]; Pablo Rodriguez-Salgado[2,3]; Conrad Childs[2,3]; Patrick M. Shannon[2,4]; Robert J. Murphy[5,6]

1 Jacobs, 160 Dundee Street, Edinburgh, EH11 1DQ, United Kingdom
2 SFI Research Centre in Applied Geoscience (iCRAG), University College Dublin, Belfield, Dublin 4, Ireland
3 Fault Analysis Group, School of Earth Sciences, University College Dublin, Belfield, Dublin 4, Ireland
4 School of Earth Sciences, University College Dublin, Belfield, Dublin 4, Ireland
5 Earth and Ocean Sciences, Irish Centre for Research in Applied Geosciences (iCRAG), University of Galway, Ireland
6 Present address: Consulting Geologist, 6 Canal Road Lower, Galway, Ireland

Abstract

Methodologies for storage assessment developed for basins with dense data coverage are typically not optimally applicable to underexplored sedimentary basins. To address this, a methodology and workflow for storage assessment in underexplored basins is presented which uses existing datasets to identify structural traps and populate a fluid-in-place equation which can be used for a variety of gases including CO_2 and H_2. This is then applied to the Irish Atlantic margin; Jurassic, Triassic and Carboniferous reservoirs are investigated to understand their reservoir quality and extent, and related seals. Structural trap types are described and the theoretical capacities of three candidate sites with varying data coverage are calculated. The results highlight the potential for underexplored sedimentary basins on the Irish Atlantic margin to support offshore renewable energy projects and reduce Ireland's CO_2 emissions. This workflow is applicable to a variety of underexplored sedimentary basins and emphasises the utility of legacy hydrocarbon datasets for early-stage subsurface storage assessment. Other aspects of energy storage are also discussed, including man-made salt caverns, other candidate reservoir-seal pairs, and the potential for collaborative infrastructure development with CO_2 emitters and renewable energy projects.

1. Introduction

There is a growing recognition of the need to reduce the release of carbon dioxide (CO_2) to the atmosphere in order to mitigate the impact of climate change, and to support the development of renewable energy sources by storing non-polluting energy vectors. Many sedimentary basins which host prolific hydrocarbon resources are now being reassessed for their potential role as subsurface storage sites, including the North Sea and the Gulf of Mexico (Holloway *et al.*, 2006; Godec *et al.*, 2011; Agartan *et al.*, 2018). This is being done using data originally collected for the exploration and development of hydrocarbon resources, now repurposed to characterise subsurface storage sites. Subsurface storage is recognised and acknowledged as a key component in the reduction of atmospheric concentrations of CO_2 (Metz *et al.*, 2005; IPCC 2022) and also represents a technologically proven method to capture excess energy generated by renewable sources as rapidly deployable kinetic energy using compressed air energy storage (CAES) or as gaseous fuels such as hydrogen (H_2) (*e.g.* Takahashi *et al.*, 2009; Lech *et al.*, 2016; Ramos *et al.*, 2021).

The two basins mentioned above host prolific petroleum systems and have been the focus of intense hydrocarbon exploration and extraction activities for several decades. Methodologies for subsurface storage assessment have been developed for these basins which typically rely on dense grids of wells and 3D seismic reflection data (*e.g.* Lloyd *et al.* 2021). These workflows are not optimally applicable to the greater number of underexplored sedimentary basins which typically have far less well data and limited 3D seismic reflection data coverage. To remedy this, a methodology and workflow is presented in this study, tailored for subsurface storage assessment in basins with more limited data coverage. It uses existing subsurface datasets in the form of well and seismic reflection data to populate an industry-standard Fluid-in-Place equation for different fluids including CO_2 and H_2.

This study outlines a methodology for estimating subsurface storage volumes in structural traps which can be applied to sedimentary basins with a range of data coverage, from high-density 3D to low density 2D grids of seismic reflection data and accompanying borehole data. This workflow is applied to three underexplored sedimentary basins offshore north-western Ireland. The lithological units which make up the most promising storage candidates within these basins are characterised and assessed for their potential as energy or CO_2 storage reservoirs. Storage structure types observed within the study area are then described, and the volumetric assessment workflow is then applied to three candidate storage sites with varying levels of data coverage, from 3D seismic reflection and dense well data coverage to low density 2D seismic lines and sparse well data. Finally, we discuss additional reservoirs on the Irish Atlantic margin which may warrant further study, briefly compare the geology of the Irish Atlantic margin to the basins offshore southern and eastern Ireland and discuss possible synergies with offshore renewable infrastructure development. In order to be applicable to multiple fluid types, this study focuses on structural traps. Although CO_2 can be stored in saline aquifers without a defined closing contour, H_2 requires structural closure (Ringrose, 2020). The workflow and methodology do not take aquifer seal capacity and connected aquifer volume into account due to this focus as an initial screening methodology for multiple fluid types, but these should be considered should the screening focus narrow to just CO_2 storage.

The results build upon previous assessments of both the hydrocarbon prospectivity (*e.g.* Trueblood, 1992; Spencer and MacTiernan, 2001; Scotchman *et al.*, 2018) and carbon dioxide storage potential (e.g. Lewis et al., 2009) of the principal Irish Atlantic margin basins with a thorough analysis of the different reservoir formations and the identification of multiple potential structural storage sites worthy of further investigation. The workflow can also be applied to other basins offshore Ireland and further afield, particularly in locations with more limited subsurface data coverage. The method is best used in early-stage screening studies when a basin is being considered for subsurface storage and it can aid offshore developers to identify synergies with infrastructure like wind farms. Renewable energy planning and development is at a nascent stage offshore Ireland (Lange *et al.*, 2018; Roux *et al.*, 2022); the results of this study will ensure policy makers, renewable energy developers and power providers have a better understanding of the opportunity potential that lies beneath the seabed.

2. Subsurface Storage

There are many economic and societal reasons for storing fluids in the subsurface. This study focuses on two uses:

- Reduction of atmospheric concentrations of CO_2 through capturing the greenhouse gas and storing it in subsurface reservoirs over geological timescales.
- Storage of energy, typically during periods when generation exceeds demand, which can be readily accessed as demand increases.

These are explored in more detail below.

2.1. CO_2 Storage

CO_2 can be captured using a variety of techniques, including directly at high-intensity sources like thermal power stations and cement plants, or from the atmosphere in lower concentrations using Direct Air Capture (DAC) methods (Bui *et al.*, 2018; Ringrose, 2020). CO_2 storage in the subsurface has been proposed as an enabler of a smoother energy transition by capturing the emissions from gas-fired power stations or cement plants without emitting them to the atmosphere (*e.g.* Lau *et al.*, 2021). There are several ways to store CO_2 underground, including precipitating it in a solid carbonate mineral such as calcium carbonate ($CaCO_3$) in basaltic rocks (*e.g.* Pogge von Strandmann *et al.*, 2019) or storing it as a fluid in saline aquifers, depleted oil and gas fields or in other structural traps (*e.g.* Bickle, 2009; Eiken *et al.*, 2011; Ringrose, 2020; Osmond *et al.*, 2022). Enhanced oil recovery (EOR) is currently the most common form of CO_2 storage in the subsurface, where it is injected to repressure reservoirs and displace hard-to-access oil accumulations (Blunt *et al.*, 1993; IEA, 2018). This study will focus on the storage of CO_2 as a fluid in structural traps (Fig. 1A).

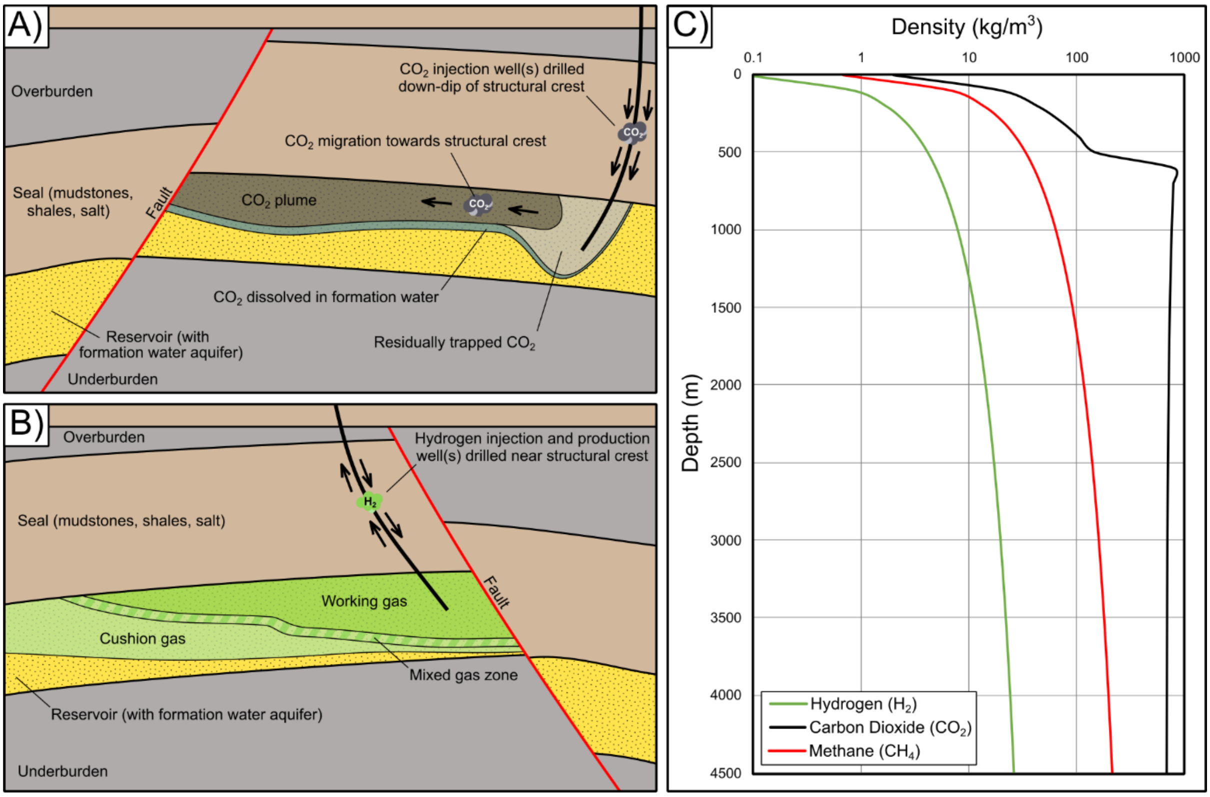

Figure 1: A) Schematic overview of CO_2 storage in structural traps. B) Schematic overview of H_2 storage in structural traps. C) Density changes of H_2, CO_2 and CH_4 (natural gas) with increasing depth. Calculated using correlations from Lindstrom and Mallard (2022), the geothermal gradient of the Slyne Basin (31°C/km), and a hydrostatic pressure gradient (100 Bar/km).

CO_2 is typically stored at depths greater than 800-1000m underground. At these depths the ambient temperature and pressure is above the critical point of CO_2 (31°C and 73-74 bar) which makes CO_2 a supercritical fluid (Ringrose, 2020). In this supercritical state CO_2 behaves in a unique way, with properties of both a liquid and a gas. Crucially, it has a much higher density than at atmospheric conditions (Fig. 1C), meaning a greater amount of CO_2 can be stored in the same volume at depth than on the surface. Supercritical CO_2 also has the viscosity of a gas, meaning it can flow into and through a porous storage medium more easily (Bui *et al.*, 2018; Ringrose, 2020). To have a meaningful impact on the effects of climate change, CO_2 must be stored in this manner for long periods of time (typically 10,000+ years) with reasonable guarantees of storage integrity (Metz *et al.*, 2005; Bui *et al.*, 2018; IPCC 2022).

There are several CO_2 storage projects which are either active or being developed at the time of writing. CO_2 associated with the original hydrocarbon accumulations has been reinjected into the subsurface at both the Sleipner and Snøhvit fields in the North Sea to avoid CO_2 release into the atmosphere (Eiken *et al.*, 2011). There are also several projects being actively developed across Europe focusing solely on CO_2 storage. These include the Northern Lights project in Norway, the Greensands project in Denmark, the Porthos project in the Netherlands, and the Acorn and Viking projects in the UK. These are located in the sedimentary basins of the North Sea; some aim to utilise decommissioned oil and gas fields such as the West Siri field for the Greensands project, while others are targeting undrilled structures or those previously found to contain no hydrocarbons, such as the Northern Lights project (Lothe *et al.*, 2019). Recent reports evaluating several active CO_2 capture projects have indicated that several flagship projects, mostly designed to sell captured CO_2 for EOR in North America, have failed to meet their annual storage targets due to either continued engineering challenges or a decrease in demand for CO_2 for use in EOR due to a fall in oil prices (*e.g.* Robertson and Mousavian, 2022). These authors also highlight the importance of robust regulatory systems such the CO_2 tax and emissions quotas employed in Norway alongside reasonable storage project economics to ensure long-term success.

2.2. Energy Storage

Energy storage involves capturing and storing energy so that it can be used at a later time. Capturing energy generated during periods of low demand to be used later during periods of higher demand is an effective way to meet energy demand, balance input to national grids and ensure security of supply. With the increasing adoption of cleaner renewable energy, such as wind and solar which are inherently variable in their supply, comes a requirement for reliable and rapidly deployable back-up sources of energy. At present this is met primarily by natural gas supplies. However, the excess energy generated by renewable sources at times when demand is lower currently goes unused. With appropriate energy storage technologies and reservoirs, this excess energy could be stored for later use when demand exceeds wind, wave, or solar energy production.

The grid-scale energy storage technologies with the greatest capacity currently in operation are pumped-storage hydroelectric dams. Hydroelectric energy storage requires suitable topography and a source of water (Edwards, 2003). Other grid-scale storage solutions include large chemical batteries, but these require a significant supply of raw-materials, often sourced through environmentally damaging and exploitative processes (Wall *et al.*, 2017), and are currently capable of providing power for only a few hours at most. Alternatively, energy can be stored in the form of fluids in subsurface reservoirs. Currently, natural gas is the most commonly stored fluid in subsurface reservoirs. In Ireland, the Southwest Kinsale gas field in the North Celtic Sea Basin was used as a storage facility for natural gas between 2001 and 2017 but has since been decommissioned (PSE Kinsale Energy, 2022).

In a similar manner to natural gas storage, other gaseous fuels can be generated using excess renewable energy and stored underground for later combustion, in a method known as Power-to-Gas (P2G). Several fluids have been proposed for this purpose, including hydrogen (H_2) and ammonia (NH_3). This study will focus on hydrogen. Hydrogen is commonly categorised into a series of colours based on how it is produced (Dincer, 2012; Dawood *et al.*, 2020; Newborough and Cooley, 2020). The most common colours are listed below:

- Grey hydrogen: produced using steam methane reforming, where water vapour (H_2O) is combined with natural gas (CH_4) at high pressures in the presence of a catalyst to produce hydrogen and carbon monoxide (CO). Further reaction occurring between the carbon monoxide and water vapour in a water-gas shift reaction produces additional hydrogen and carbon dioxide (CO_2). This is currently the most common production method (IEA, 2022).
- Blue hydrogen: produced using the same methods as grey hydrogen but the CO_2 is captured and stored rather than being emitted.
- Green hydrogen: produced using renewable energy to power the electrolysis of water (H_2O) to produce hydrogen and oxygen (O_2).

In the case of green hydrogen both the production and combustion of this gas produces no CO_2, highlighting its potential to decarbonise power generation (Dincer, 2012). However, while hydrogen has a higher energy content than natural gas, it is significantly less dense (Heinemann *et al.*, 2018). Therefore, significant subsurface storage volume would be required to meet grid-scale energy demand currently provided by fuels like natural gas (Heinemann *et al.*, 2018; Crotogino, 2022; Duffy *et al.*, 2023). Its lower density also makes hydrogen more buoyant than formation water in subsurface sandstone reservoirs, leading to it migrating towards the surface unless stored in a structural trap (Fig. 1B). Other properties of hydrogen, including its diffusivity, smaller molecular size and wettability properties indicate the importance of detailed seal characterisation when planning to store this fluid in structural traps (Iglauer, 2022; Miocic *et al.*, 2023).

3. Dataset and Methodology

3.1 Dataset

The significant amount of subsurface data that was collected by a variety of companies in the search for hydrocarbon accumulations (Naylor, 1983; Shannon, 2018) can be used to understand the storage potential of different reservoir formations in the Slyne, Erris and Donegal basins. These basins are chosen as the focus for the present study as they lie relatively close to the Irish mainland and are in somewhat shallower water by comparison to other basins off the west coast of Ireland, such as the larger, more oceanward Porcupine and Rockall basins (Fig. 2). The database comprises seismic reflection data, variably tied to exploration, appraisal and development wells and shallow boreholes. The 2D seismic database consists of 25 surveys acquired between 1975 and 2014 which total over 49,000 km in line-length (Fig. 2). The 3D seismic database consists of 12 surveys, acquired between 1997 and 2013, covering a total area in excess of 6000 km^2, although there is some survey overlap in the Northern Slyne sub-basin (Fig. 2). Some of these surveys were reprocessed in 2006, 2012 and 2018. Seismic data is presented in European polarity, where a downward decrease in acoustic impedance corresponds to a negative (blue) reflection event and an increase in corresponds to a positive (red) reflection event. Seismic and geoseismic sections are vertically exaggerated by a factor of three. In the geoseismic sections, ball-ends are used to highlight where a fault terminates within a certain stratigraphic package, while faults without ball-ends are truncated by a younger surface.

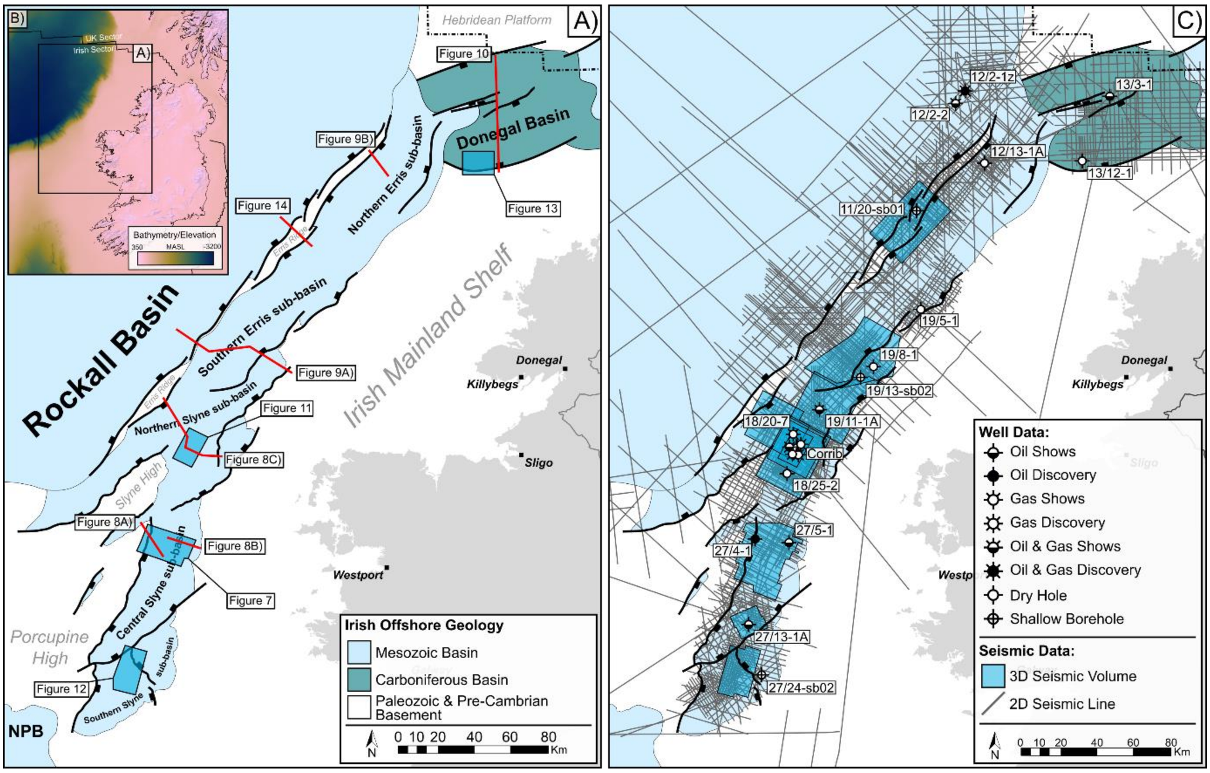

Figure 2: Overview map of the study area. A) Map showing the distribution of basins offshore north-western Ireland. Abbreviations: NPB – North Porcupine Basin. B) Bathymetry around the island of Ireland. Abbreviations: MASL – Metres Above Sea Level. C) Map showing the distribution of borehole and seismic reflection data used in this study.

The geology of the seismic database was constrained using exploration, appraisal, and production wells from the Slyne, Erris and Donegal basins. This includes two wells in the Donegal Basin, two wells in the Erris Basin, and 15 wells in the Slyne Basin. Data from these wells includes wireline logs, formation tops, lithological descriptions, temperature, and pressure data from well reports and composite logs, and core data where available. The most recent stratigraphic nomenclature and biostratigraphy were used for this study, derived from the updated stratigraphic database for offshore Ireland (Merlin Energy Resources Consortium, 2020).

3.2. Methodology

3.2.1 Regional mapping and structure identification

Geological formations with a significant porous and permeable sandstone content represent ideal energy and CO_2 storage candidates. Three sandstone reservoir formations are analysed in the study area, based on their previous identification as hydrocarbon exploration targets (*e.g.* Dancer *et al.*, 2005): Carboniferous, Lower Triassic, and Upper Jurassic reservoirs. These reservoir horizons were mapped throughout the study area, to create regional structure maps and to understand their distribution. To identify structural closures and measure gross rock volumes, they were then converted from the time domain to the depth domain using velocity models. The depth conversion model used interval layers defined by two-way-time mapping of the seabed, Base Cenozoic, Base Cretaceous, Base Upper Jurassic, Top Triassic, Top Lower Triassic, Top Permian and Base Permian horizons. An initial velocity (V_0) and *k*-factor (the change in velocity with increasing depth) were calculated for each interval using well-derived time-depth relationships (Table 1). Due to the variable structural development across the study area, certain intervals were absent in some of the sub-basins.

Table 1: Values used to depth convert 3D reservoir surfaces. Values derived from well-based velocity data.

Stratigraphic interval	**V_0 (ms^{-1})**	***k***
Water column (surface to seabed)	1468-1500	N/A
Cenozoic	1510-1579	N/A
Cretaceous	2756-2970	N/A
Upper Jurassic	2440-2483	0.50
Lower and Middle Jurassic	2750-3200	0.25-0.40
Upper Triassic	4400-4822	0.15-0.20
Lower Triassic	4800-5000	0.15
Permian	5000	N/A
Carboniferous	5100-5422	0.10

The regional top reservoir maps were then used in a spill-point analysis to identify structural traps throughout the study area (Møll Nilsen *et al.*, 2015). This method uses nodal analysis on all the points which make up a reservoir surface to locate local maxima which represent structural closures and identifies the spill point on each closure. Depth converted reservoir surfaces were resampled to 250 m by 250 m grids to improve computation time in the spill point analysis. The spill point analysis generated polygons on these re-gridded surfaces representing the map-view outlines of structural closures. These polygons were then overlayed on the higher resolution depth converted surfaces (*i.e.* prior to resampling) to ensure the closure was valid on the more detailed surfaces. These higher resolution surfaces were then used for calculating gross rock volumes inside these polygons.

3.2.2. Calculating storage potential

The potential storage capacity of a structural trap can be calculated as Fluid In Place (FIP) using the equation below:

$$FIP = \mathrm{G}RV \times NtG \times \Phi \times S_g \times \rho_g$$

Where GRV (m^3) is the gross-rock volume, NtG (net-to-gross) is the ratio of reservoir to non-reservoir rock, ϕ is the depth-dependant porosity (*i.e.* fraction of the rock made up of void space), and S_g is the maximum fluid saturation. This represents the total pore space within a structural closure which can be occupied. This can then be multiplied by the density (ρ_g) of the fluids at reservoir conditions to understand how much of each fluid (*i.e.* CO_2 and H_2) can be stored in these structures. Values for CO_2 capacity are presented in million tonnes while H_2 values are multiplied by the higher heat capacity of hydrogen (39.4 KWh/kg or TWh/million tonnes) to better understand its grid contribution as an energy storage medium.

A final consideration for an injected fluid that is to be returned to the surface for use (*i.e.* H_2) is the requirement for a certain volume of fluid to be left in the reservoir to maintain a suitable pressure to support efficient production (termed 'cushion gas'). Therefore, only a portion of the calculated volume in any prospective storage site will constitute fluid that can be stored and withdrawn economically (Fig. 1B). The percentage of the storage volume which will be required to act as cushion gas will vary depending on the initial pressure of individual structures but will likely be between 40-60% of the total volume of a structure (McVay and Spivey, 2001; Klempa *et al.*, 2019). Therefore, the effective storage capacity of a candidate storage site (commonly termed the 'working gas volume') will be the remaining percentage of the total volume:

$$Working\ Gas\ \% = 100\% - Cushion\ Gas\ \%$$

The data and techniques used to populate each of the inputs to the FIP equation are expanded upon in the following sections. This includes both the data available for this case study of the Irish Atlantic margin alongside more general inputs, when applying this methodology to other sedimentary basins.

3.2.3. Gross rock volume (GRV)

Gross rock volume was determined by calculating the volume between the top and base of the reservoir section above the spill point on that structure. Volumes were calculated between the top and base depth-converted regional reservoir surfaces down to the spill point for that structural closure. If the base reservoir surface was above the spill point contour, the volume of non-reservoir rock below the base of the reservoir, but above the structural spill point, was subtracted from the GRV. In the case of the Corrib gas field, which was not fill-to-spill upon discovery, two volumes were calculated, one representing the initial Free Water Level and the other representing the spill point of the structural closure. If less data are available, it may be possible to use the volumes of regular shapes (*e.g.* cylinders, ellipsoids and prisms) as simplified proxies for structural traps.

3.2.4. Net-to-gross (NtG)

The ratio of the gross storage formation to reservoir-grade rock is termed the net-to-gross (NtG). The NtG of each of the three storage formations evaluated in this study was calculated in each well by measuring the thickness of reservoir-grade rock and calculating the ratio of this thickness to the total thickness of the reservoir section in that well. Net reservoir was defined using a Vshale curve derived from the gamma logs (Asquith *et al.*, 2004). The Vshale curves were then compared with cuttings and core descriptions included in well completion reports and composite logs to ensure that suitable sand and shale cut-offs were accurately representing the geology in the wells.

Given the variable diffusivity of the gases being studied (*i.e.* CO_2 and H_2) it is best to define different Vshale cut-offs given the expected permeability for each of the facies being defined. However, one cut-off was used for this study to simplify calculations. The NtG values from each well were then extrapolated across the study area to produce predictive NtG maps for each of the storage plays. Due to the sparse point data (typically 10s of kilometres between wells), ordinary kriging was used to interpolate between data points. If no NtG data is available, it may be possible to estimate variations in NtG based on expected reservoir facies using outcrop analogues. In the case of the Slyne and Erris basins offshore northwest Ireland, the data-rich East Irish Sea Basin would be a suitable analogue.

3.2.5. Porosity (ϕ)

Porosity data for each of the key storage formations is relatively limited given the few wells drilled in the study area. This data is primarily derived from wireline porosity logs, core, and core plug analysis included with well completion reports. In data poor areas, like underexplored sedimentary basins, predictive tools can be used to supplement what data does exist. Porosity decreases with increasing burial depth primarily due to mechanical compaction. Empirical compaction curves have been developed for several different regions and lithologies which describe the change in porosity with depth and can be applied to the reservoir formations on the Irish Atlantic margin. Sclater and Christie (1980) demonstrated that porosity at depth (ϕ_z) can be estimated using the equation below:

$$\phi_z = \phi_0(e^{-cz})$$

Where ϕ_0 is the porosity at the surface, c is the porosity-depth coefficient and z is depth.

Due to the geology of the sedimentary basins analysed in this study, this standard equation was modified to account for severe uplift and erosion that have impacted the reservoir formations (Chapman *et al.*, 1999; Dancer *et al.*, 1999). Failure to consider the impact of this erosion could lead to overestimation of the porosity and therefore the capacity of potential storage sites. The magnitude of erosion varies throughout the basin from a few 100s of metres to multiple kilometres (Corcoran and Clayton, 2001; Biancotto *et al.*, 2007; O'Sullivan *et al.*, 2022). Porosity values recorded from core, core plugs and wireline data for the three storage plays do not follow the typical mechanical compaction curve of Sclater and Christie (1980) as these sandstones have undergone greater compaction due to burial during rifting prior to being exhumed during the Cretaceous and Cenozoic (Fig. 3). Shifting the empirical compaction curves vertically by the magnitude of erosion, so that it aligns with borehole data corrects for this phenomenon. This has been done previously by Corcoran and Mecklenburgh (2005) using data from the Lower Triassic reservoir to study the magnitude of exhumation of the Corrib gas field and is expanded here to include additional data and reservoirs.

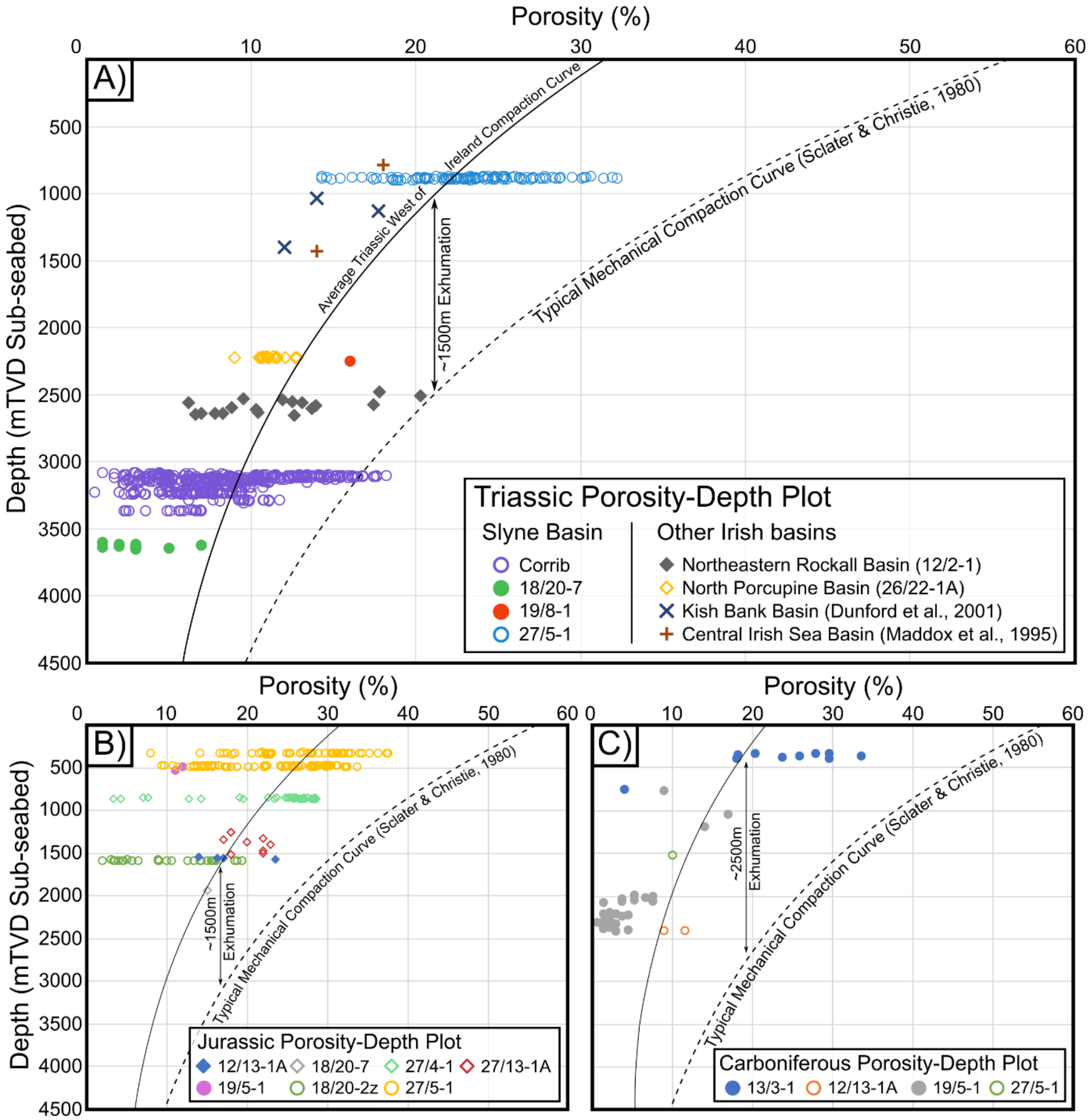

Figure 3: Porosity-depth plots for the three storage plays investigated in this study. A) Lower Triassic, B) Upper Jurassic and C) Carboniferous. Triassic reservoir details from the Kish Bank Basin and Central Irish Sea Basin are taken from Dunford et al. (2001) and Maddox et al. (1995) respectively.

3.2.6. Fluid saturation (S_g)

Not all existing formation water can be displaced when either H_2 or CO_2 is injected into a water-saturated porous subsurface reservoir. This is caused by the relative permeabilities of different fluid components (*e.g.* water and CO_2 or water and H_2). Therefore, only a fraction of the total pore space will be occupied by the injected fluid. Several laboratory studies have been carried out in recent years to investigate the relative permeability and theoretical range of fluid-saturations for CO_2 and H_2 stored in subsurface sandstone reservoirs (*e.g.* Krevor *et al.*, 2012; Yekta *et al.*, 2018; Hashemi *et al.*, 2021; Rezaei *et al.*, 2022; Thiyagarajan *et al.*, 2022) which indicate a fluid saturation range of 0.2 to 0.65. These values provide upper and lower limits for fluid saturation values during volume estimation.

It should be noted that H_2 has only been stored in artificial salt caverns in the subsurface to date. The understanding of the multiphase fluid dynamics of H_2 in porous mediums like sandstone reservoirs in the subsurface is at an early-stage relative to that of CO_2 and oil and gas. Therefore, the saturation values here represent current lab-based results (*e.g.* Yekta *et al.*, 2018) and will likely be refined with further research.

3.2.7. Fluid density (ρ_g)

The density of a fluid changes with temperature and pressure, both of which increase with increasing depth beneath the Earth's surface. These densities were calculated using correlation tables based on equations of state for individual fluids (*e.g.* Span and Wagner, 1996). Correlations from Lindstrom and Mallard (2022) were used in this study.

Predictive pressure and temperature values for calculating fluid densities at reservoir depths were generated using data from exploration wells in the study area. Plotting corrected temperature readings for wells throughout the study area indicate a regional geothermal gradient of 31 °C/km (Fig. 4A). Pressure data are only available for wells in the Slyne Basin, where most wells have encountered a near-hydrostatic pressure gradient of 0.1 Bar/m or 10,000 Pa/m throughout the drilled section (Fig. 4B), including those with breached oil accumulations (*e.g.* the Upper Jurassic reservoirs in the 18/20-1, 27/5-1 and 27/13-1A wells). While no pressure information is available from wells in the Erris or Donegal basins, no indicators of overpressure were encountered in any of the wells drilled in those basins. Therefore, a hydrostatic pressure gradient can be used to reasonably predict pressure changes with depth in these basins.

The main exception to the absence of overpressure indication is the Lower Triassic reservoir section of the Corrib gas field in the Northern Slyne Sub-basin which is modestly overpressured by 45 Bar (c. 650 psi) relative to the regional hydrostatic gradient (Fig. 4C). This may be caused by the overlying Upper Triassic salt preserving higher pressure during exhumation (Corcoran and Doré, 2002). No direct pressure information is available for the two other structures which encountered the same Lower Triassic reservoir overlain by Upper Triassic salt (wells 18/20-7 and 19/11-1A), although log-derived pressure estimations from the 19/11-1A well suggests it encountered a similarly overpressured reservoir to the Corrib aquifer in the Lower Triassic reservoir (Statoil, 2004). In wells where the Upper Triassic seal is composed of mudstone rather than salt (*e.g.* wells 19/8-1 and 27/5-1), the Lower Triassic reservoir is normally pressured (Enterprise, 1996a; StatoilHydro, 2009). Due to the general lack of pressure data, our workflow does not consider pressure limitations or address the mapping or estimation of pressure cells surrounding the structural closures. Nevertheless, it should be noted that structural and depositional barriers and baffles to pressure will have a significant impact on injectivity and, in the case of H_2, also in production flow rates, water-cut and ultimate recovery factor.

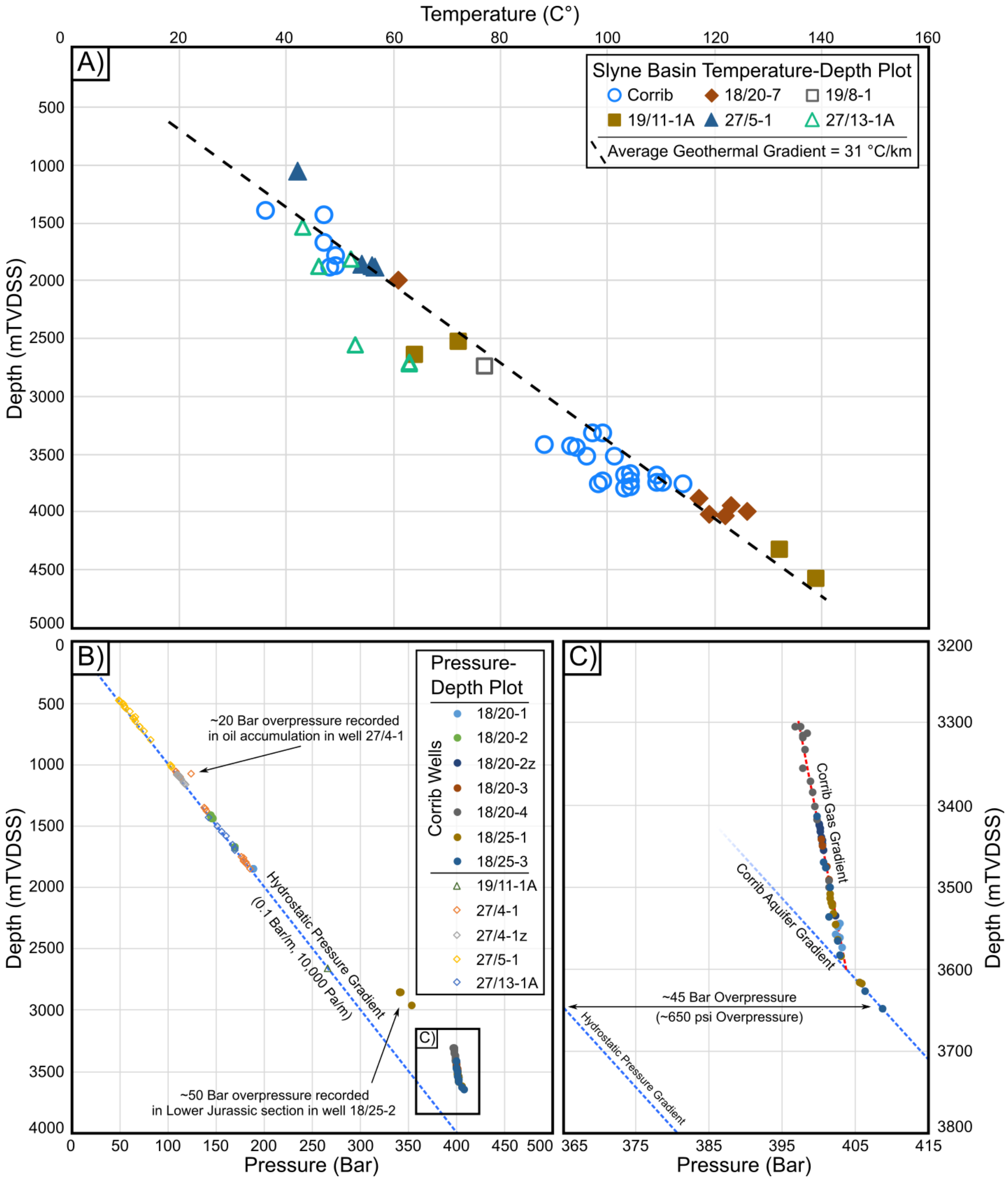

Figure 4: A) Temperature-depth plot for corrected down-hole temperature measurements from the Slyne Basin. B) Pressure-depth plot for all wells in the Slyne Basin. C) Pressure-depth plot for all data from the Lower Triassic section in the Corrib gas field.

3.2.8 Additional factors for CO_2 storage (storage efficiency and aquifer volume)

While this methodology and workflow has been presented to be suitable for different fluid types (*i.e.* both CO_2 and H_2), should focus narrow to just subsurface CO_2 storage then there are additional factors to consider. This includes both the storage efficiency factor, and the total aquifer volume and aquifer seal capacity which captures the continuity of the aquifer and how pressure changes might impact regional seal integrity.

The storage efficiency factor is introduced into volumetric calculations to account for a variety of factors including the fluid dynamics of CO_2, reservoir and seal properties, and variations in well design and injection rates (Bachu, 2015). This factor is typically added as an additional variable in the FIP equation to calculate 'effective capacity' rather than the 'theoretical capacity' represented by the standard FIP equation. This factor has been found to be very site specific with values ranging from 0.005 to >0.1 (Bachu, 2015; Ringrose, 2020). The Sleipner CCS project offshore Norway has achieved a storage efficiency of about 5% (*i.e.* a storage efficiency factor of 0.05) after two decades of operation (Ringrose, 2018). As the method used in this study is designed to be applicable for various fluid types (*i.e.* both CO_2 and H_2) this was not included in volumetric calculations but can be easily introduced into the FIP equation for studies focused solely on CO_2 storage. It is likely that a single storage efficiency factor would be used when building an inventory of storage sites across a sedimentary basin prior to ranking, with the storage efficiency factor being refined with reservoir modelling for the shortlisted storage sites. It is likely that a similar efficiency factor will be derived for H_2 storage in porous sandstone reservoirs, but as research into the fluid dynamics of H_2 in the subsurface is relatively nascent when compared with hydrocarbons and CO_2, a theoretical storage estimate is suitable for now.

Taking the total volume of the aquifer connected to a storage site is important when considering the feasibility of regional injection of fluids into the subsurface. As CO_2 is injected into a porous medium it will displace the existing fluids and increase pressure in front of the growing plume of injected CO_2. This could lead to overpressure and breakdown of the regional seal for the reservoir leading to escape of CO_2 to the atmosphere. Modelling, tracking and management of pressure changes due to CO_2 injection is therefore critical to project success and this is becoming apparent in basins where multiple independently operated CO_2 storage projects are planned, such as the basins of the Southern North Sea (Agada *et al.*, 2017). Therefore, reservoir simulations should be created to model planned injection volumes and rates to understand both local and basin-scale pressure changes, identify potential areas of excess pressure build-up, and modify these injection strategies accordingly. These considerations will have to be considered for subsurface H_2 injection as well, as this fluid displaces the existing brine within the porous sandstone formation.

3.2.9 Storage structure ranking

While not carried out in this study, a final step in selecting suitable sites for further investigation would be a quantitative ranking scheme. Studies have looked at the application of a variety of multi-criteria ranking schemes to geospatial site ranking (including for CO_2 storage siting) using techniques such as Quantitative Strength, Weakness, Opportunities, and Threats (SWOT) and Technique for Order of Preference by Similarity to Ideal Solution (TOPSIS) analyses (*e.g.* Alcalde *et al.*, 2021; Chock *et al.*, 2022). Criteria should include geological factors such as porosity, seal lithology, and depth and could also consider non-geological factors like distance from shore, proximity to major CO_2 emitters or energy customers, and presence of existing infrastructure. For projects focused purely on CO_2 storage, aquifer seal capacity and total connected aquifer volume should also be considered.

4. Geological Setting

The Slyne, Erris and Donegal basins, located offshore north-western Ireland, have been the subject of intermittent hydrocarbon exploration and development for over 50 years (Trueblood, 1992; Scotchman and Thomas, 1995; Shannon and Naylor, 1998; Scotchman *et al.*, 2018). They are a group of broadly contiguous basins located 30-60 kilometres off the north-western coast of Ireland in water depths of 150-3000m (Fig. 2). The basins are elongate and fault-bound, bordered by the crystalline rocks of the Irish Mainland Shelf to the east and the Erris Ridge and Porcupine High to the west, and belong to a framework of basins of various ages and structural styles which stretch across the Irish Atlantic margin (Fig. 2).

4.1. Tectonostratigraphic evolution

The geology of the study area is a product of a complex geological evolution extending from the Early Paleozoic to the present day (Chapman *et al.*, 1999; Dancer *et al.*, 1999; O'Sullivan *et al.*, 2022). The oldest rocks investigated in this study are Carboniferous strata deposited in several fault-bound basins which formed during back-arc extension as the Rheic Ocean was subducted beneath the Laurentian continent (Woodcock and Strachan, 2012). These include a predominantly marine Mississippian sequence of limestones, sandstones and mudstones overlain by a terrestrial Pennsylvanian sequence of mudstones, sandstones and layers of coal (Fig. 5; Tate and Dobson, 1989). These Carboniferous basins were locally inverted by compressional forces associated with the Variscan Orogeny (Worthington and Walsh, 2011). Alongside local inversion, regional uplift and erosion created the Variscan Unconformity.

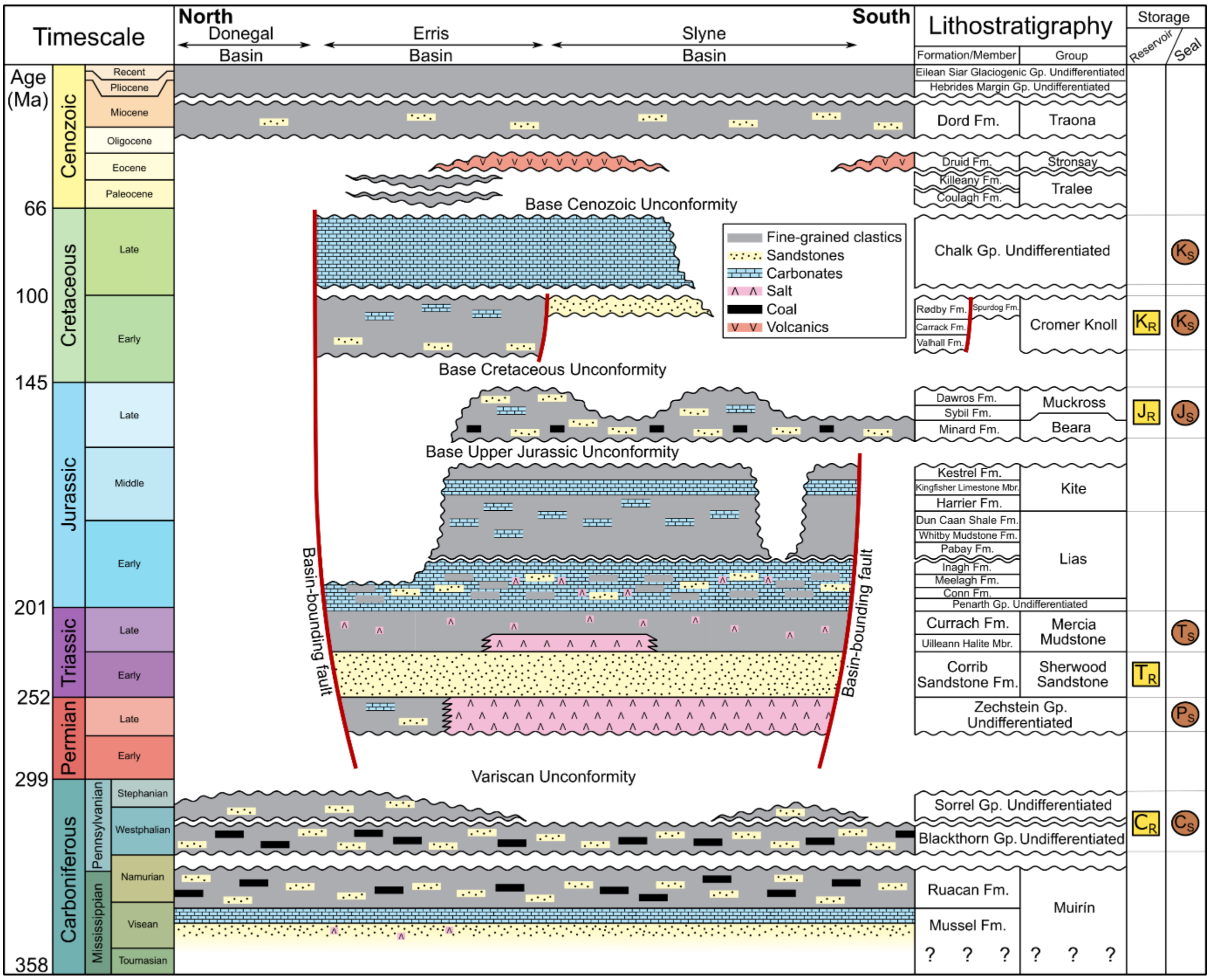

Figure 5: Stratigraphic column for the Slyne, Erris and Donegal basins. The key storage plays are highlighted. The stratigraphic nomenclature is adapted from Merlin Energy Resources Consortium, (2020).

Post-orogenic extension began in the Late Permian, accompanied by the formation of several hundred metres of salt in the hanging walls of active faults alongside thin carbonate and clastic deposits on intrabasinal highs (Doré *et al.*, 1999; O'Sullivan *et al.*, 2021). This was followed by a period of tectonic quiescence during the Early and Middle Triassic, with the development of braided river systems in an arid environment throughout the study area (Dancer *et al.*, 2005). This was overlain by red mudstones deposited in sabkha and playa lake environments, and locally a second layer of salt, representing an ephemeral marine incursion, during the Late Triassic (Merlin Energy Resources Consortium, 2020). There is also evidence of regional extension and halokinesis initiating during the Late Triassic period (O'Sullivan and Childs, 2021).

A second period of regional extension occurred during the Early and Middle Jurassic in tandem with a marine transgression. A sequence of marine limestones, mudstones and sandstones was deposited throughout the region, thickening into the hanging walls of active faults (Dancer *et al.*, 1999). Several salt structures formed during the Early to Middle Jurassic, including salt anticlines, rollers and walls (O'Sullivan *et al.*, 2021; O'Sullivan and Childs, 2021). Early and Middle Jurassic extension ceased during the late Middle Jurassic when the region experienced uplift and erosion (Dancer *et al.*, 1999). The exact cause of this uplift and erosion is poorly constrained but may be related to a mantle plume in a similar but less severe manner to the North Sea doming event (Ziegler, 1992).

A third extensional phase began during the Late Jurassic, accompanied by kilometre-scale movement on the basin-bounding faults and the deposition of a thick sequence of fluvio-estuarine mudstones and sandstones throughout the study area (Dancer *et al.*, 1999; O'Sullivan *et al.*, 2022). A second phase of halokinesis occurred in tandem, with new structures being formed and pre-existing structures created in the Early and Middle Jurassic being reactivated and modified (O'Sullivan *et al.*, 2021). A marine transgression occurred towards the end of the Jurassic, with the uppermost Jurassic sediments consisting of marine limestones and mudstones (Merlin Energy Resources Consortium, 2020).

Most of the study area experienced kilometre-scale uplift and erosion during the Early Cretaceous, creating a distinct regional unconformity. This was driven by rifting and hyperextension in the neighbouring Rockall Basin to the northeast (Fig. 2). The Erris Basin is a notable exception and was involved in the extension of the Rockall Basin, with over a kilometre of predominantly marine sediments accumulating in this basin during the Cretaceous (Chapman *et al.*, 1999; O'Sullivan *et al.*, 2022). Several structures underwent subtle modification and reactivation during this period of exhumation, with small reverse and normal movements on faults observed throughout the study area (Corcoran and Mecklenburgh, 2005; O'Sullivan *et al.*, 2022).

The area experienced additional periods of uplift during the Cenozoic, which are variously attributed to the Alpine Orogeny, the development of the Icelandic plume and the onset of oceanic crust formation and associated ridge-push in the North Atlantic Ocean (Dancer *et al.*, 1999). The magnitude of uplift was less severe than that experienced in the Early Cretaceous, with a few hundred metres of sediment removed (Corcoran and Mecklenburgh, 2005). Several structures underwent further modification and reactivation during the Cenozoic as a result of these post-rift tectonic processes (O'Sullivan *et al*., 2022). Regional magmatism occurred during the Cenozoic, with the intrusion of igneous sills and dykes throughout the Carboniferous and Mesozoic rocks, and the extrusion of lavas over certain parts of the study area (Dancer *et al.*, 2005; O'Sullivan and Childs, 2021). Following the extrusion of these Cenozoic lavas, marine and glaciogenic mudstones and sandstones were deposited throughout the study area during the Cenozoic. Finally, glaciation during the Pleistocene impacted the basins offshore western Ireland, with the British and Irish Ice Sheets (BIIS) extending from the present-day coastline across the Malin Shelf, Irish Mainland Shelf, and the eastern margins of the Slyne and Erris basins (Clark *et al.*, 2022). Glaciogenic sediments were deposited across most of the study area (Merlin Energy Resources Consortium, 2020) while glacioisostasy may have further reactivated faults or modified structures as noted in other glacially influenced basins such as the North Sea (Goffey *et al.*, 2018) although no direct evidence of this has been reported to date.

5. Storage play characterisation

Each of the reservoir units is described in terms of a 'storage play' in a similar manner to a 'petroleum play' used in hydrocarbon exploration. The methodologies used are similar to the description of petroleum plays offshore Ireland (*e.g.* Trueblood, 1992; Spencer and MacTiernan, 2001). In a petroleum play, these components include source, reservoir and seal rocks, hydrocarbon generation, migration pathways and a trap that formed prior to hydrocarbon migration. Certain components which are required in the petroleum play (*e.g.* the source rock, migration route from source to reservoir, and the timing of trap formation) are irrelevant for subsurface fluid storage and so are not considered here. Similar concepts have been applied to pure hydrogen storage and termed 'hydrogen plays' (*sensu* Heinemann *et al.*, 2018). Here we expand on this to describe subsurface 'storage plays' which can be used to store a variety of fluids including CO_2 and H_2. To achieve this, the stratigraphic nomenclature, depositional environment, regional distribution and reservoir properties including net-to-gross and porosity are described for each of the three main storage plays considered in this study. Some additional storage plays which are more poorly constrained are also discussed.

Given varying capillary entry pressure for different gasses (*e.g.* CO_2, H_2 and CH_4) some nuance is required when characterising the seals of these storage plays. Given the smaller size of H_2 molecules relative to other relevant gases, a very low permeability seal is required to effectively contain H_2 in the subsurface. Salt is best suited to this due to its very low permeability and is the only proven subsurface hydrogen storage medium at time of writing (albeit in artificial caverns within the salt). Conversely, mudstones are likely to be less effective at sealing H_2 storage sites. Therefore, some storage plays may be suitable for both H_2 and CO_2 storage, while others may only be suitable for CO_2 storage.

5.1. Carboniferous storage play (C_R)

The Carboniferous is one of the most poorly understood sedimentary sections within the study area. Being one of the deepest proven sedimentary sections in the area, it was often considered the 'economic basement' in the region, with only the upper few 10s of metres being penetrated and described in boreholes. It is also typically characterised by low-amplitude reflectors on seismic data, making regional mapping of distinct markers within the Carboniferous section rather difficult.

The most extensive Carboniferous section was encountered in the 19/5-1 well in the Erris Basin. This well encountered 1679 metres of Carboniferous strata, which can be broadly subdivided into three sections (Fig. 6A). The youngest of these are the Pennsylvanian Sorrel and Blackthorn groups, which were deposited in a predominantly coastal, deltaic and swampy environment. This section is underlain by the Muirín Group, which is subdivided into the Ruacan and Mussel formations. The Ruacan Formation was deposited in shallow marine and continental settings, while the Mussel Formation was deposited primarily in a continental environment (Merlin Energy Resources Consortium, 2020). The Ruacan and Mussel formations have only been encountered in the 19/5-1 well, while other wells which penetrate the Carboniferous terminate within the Blackthorn Group (Fig. 5). Seismic data, particularly in the Donegal Basin, indicate a thick undrilled sedimentary sequence beneath the Blackthorn Group, which may represent Muirín Group sediments. The Carboniferous section is notably absent in the 18/25-2 well in the Slyne Basin (Fig. 5A), where metasediments tentatively dated as Silurian were encountered beneath the Zechstein Group (Enterprise, 2000). This indicates that there may be other local highs within the study area where Carboniferous sediments are similarly absent.

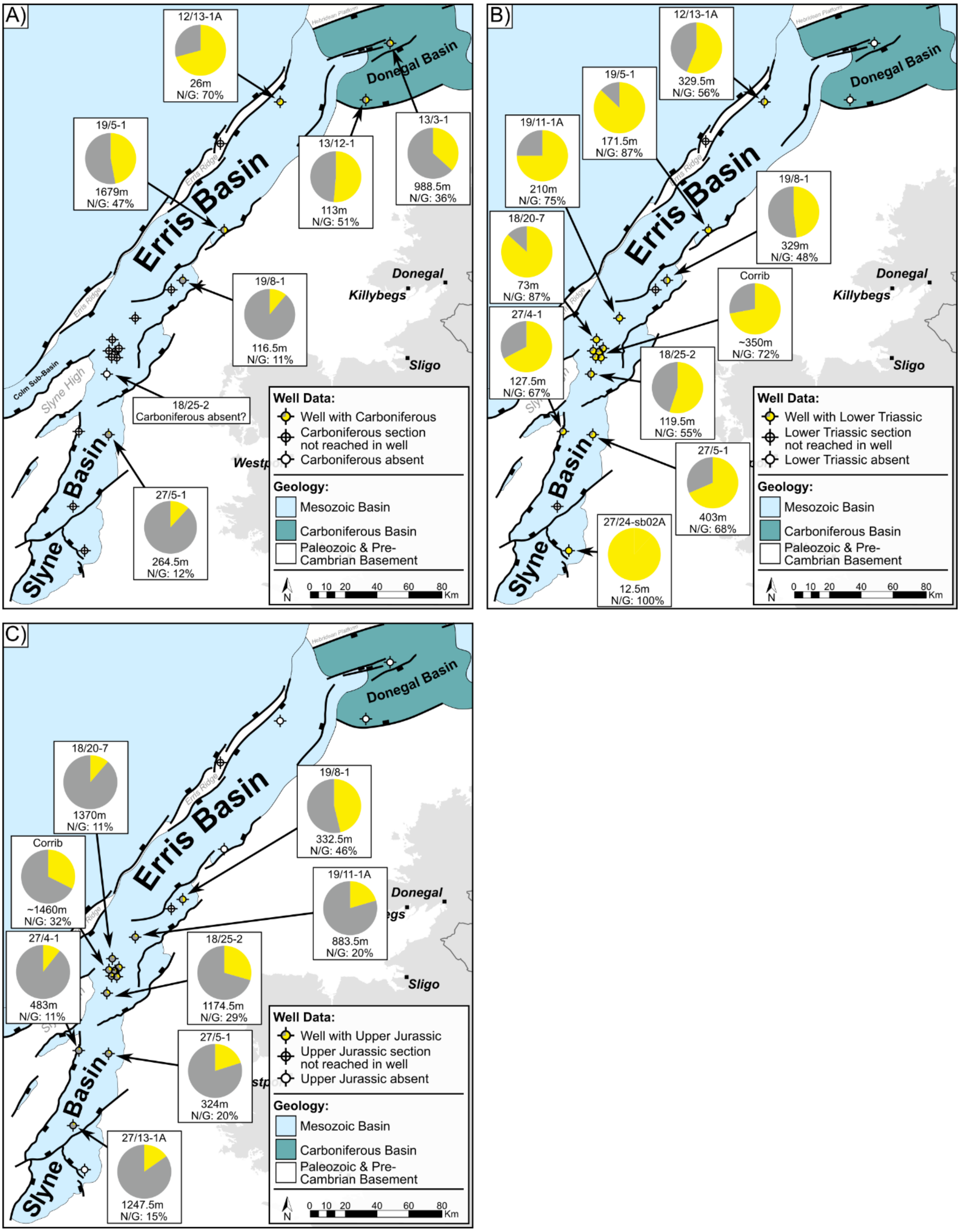

Figure 6: Maps showing the net-to-gross calculated from gamma ray log-based Vshale calculations and lithological descriptions for the A) Carboniferous, B) Lower Triassic and C) Upper Jurassic storage plays in the study area. Reservoir rock is shown in yellow while non-reservoir rock is shown in grey.

The proven reservoir-seal pairs which make up the Carboniferous storage play are the interbedded sandstones and mudstones throughout the Sorrel, Blackthorn and Muirín groups. Within the Sorrel and Blackthorn groups these reservoirs are likely to be the fluvial sandstone channels surrounded by overbank and floodplain mudstone deposits present in a deltaic depositional environment (Tate and Dobson, 1989; Merlin Energy Resources Consortium, 2020) These channelised sandstones are likely to have limited lateral extent. Conversely, the sandstones in the Ruacan and Mussel formations represent more extensive shallow marine sheet sands and continental aeolian and alluvial fan deposits respectively (Merlin Energy Resources Consortium, 2020). A broad northward increase in the net-to-gross is observed in the relatively sparse Carboniferous well data which primarily samples the Sorrel and Blackthorn groups (Fig. 6A). This may suggest a northern source for the predominantly fluvial Carboniferous reservoir sandstones and a greater sandstone content in this region.

The shallowest Blackthorn Group sandstones in the 13/3-1 well have porosities of 18-34% but this decreases to 3-5% below 500mTVD sub-seabed (Fig. 3, Texaco, 1978). Reasonable reservoir properties were observed in the Blackthorn Group in the 19/5-1 well, with porosities between 9-17% (Fig. 3, Amoco, 1978). The Ruacan Formation in the 19/5-1 well had very limited porosities no higher than 8% (Fig. 3), while the underlying Mussel Formation was described as having no porosity (Amoco, 1978). Both the 12/13-1A and 27/5-1 wells recorded similarly mediocre porosity values around 10% (Fig. 3).

The seal to these Carboniferous sandstones is provided by the mudstones interbedded with the fluvial and deltaic sandstones. These were deposited in the floodplains and swamps surrounding the fluvial and deltaic channels and are likely to be laterally extensive (Merlin Energy Resources Consortium, 2020). No hydrocarbon accumulations have been found in Carboniferous rocks within the study area to indicate if these mudstones provide an adequate seal. The lateral equivalent to this Carboniferous section in the Lough Allen Basin onshore Ireland hosts sub-commercial gas accumulations (Philcox *et al.*, 1992), which suggests the similar mudstones present in the study area could provide an effective seal. Conversely, the presence of gas-charged Cenozoic sediments and seabed pockmarks in the Donegal Basin (Garcia *et al.*, 2014), where the Carboniferous section lies directly beneath the Base-Cenozoic Unconformity, may indicate that cross-fault mudstone-sandstone juxtaposition does not provide an effective seal. Therefore, detailed fault seal analysis will be needed for structural traps which rely on fault offset for closure.

5.2. Lower Triassic storage play (T_R)

The Triassic storage play in the Slyne and Erris basins consists of the Lower Triassic Corrib Sandstone Formation, sealed by the overlying Upper Triassic Currach Formation (Fig. 5). This is the only storage play analysed at this stratigraphic level which also hosts a developed hydrocarbon reservoir (the Corrib gas field). All wells which reached the Lower Triassic section encountered the Corrib Sandstone Formation (Merlin Energy Resources Consortium, 2020).

The Corrib Sandstone Formation was deposited in a broad northeast flowing braided river system with indications of marginal areas of aeolian dune systems and playa lake deposits (Dancer *et al.*, 2005; Merlin Energy Resources Consortium, 2020). This results in very high net-to-gross values greater than 50% observed in the Corrib Sandstone Formation throughout the Slyne and Erris basins (Fig. 6B). Local variations have been noted in the 12/13-1A well in the Erris Basin where thin carbonate layers were interpreted as calcrete deposition (Merlin Energy Resources Consortium, 2020). A shallow borehole on the eastern margin of the Slyne Basin encountered a coarse-grained conglomerate, suggesting more immature and local sediment sourcing towards the basin-margins (Fugro, 1994).

Plotting porosity against depth from various wells in the Slyne and Erris basin supports the kilometre-scale exhumation interpreted by previous authors (*e.g.* Scotchman and Thomas, 1995; Corcoran and Mecklenburgh, 2005; Biancotto *et al.*, 2007). This trend indicates that the expected porosity at a certain depth should be 5-10% lower than that predicted by compaction curves from typically shaly-sandstones (*e.g.* Sclater and Christie, 1980). This estimate does not account for the variation in both burial histories and the magnitude of exhumation observed across the study area (*e.g.* O'Sullivan *et al.*, 2022); some exploration wells have encountered Triassic sandstones with better (*e.g.* 19/8-1) and poorer (*e.g.* 18/20-7) porosity values than those predicated by the modified compaction curve (Fig. 3A).

The Corrib Sandstone Formation is sealed by the overlying Upper Triassic Currach Formation. This is primarily composed of red mudstones interbedded with lenses of anhydrite which formed as regional sabkhas and playa lakes during the Late Triassic and is found throughout the Slyne and Erris basins (Merlin Energy Resources Consortium, 2020). A layer of halite (the Uilleann Halite Member, Fig. 4) is present at the base of the Currach Formation in the Northern Slyne and Southern Erris sub-basins. This has been interpreted to extend into the Central and Southern Slyne sub-basins by Merlin Energy Resources Consortium (2020), but detailed seismic mapping and well interpretation indicate it likely does not extend into these sub-basins (O'Sullivan *et al.*, 2021). This halite layer likely represents a more competent seal than the interbedded mudstones and is the seal for the Corrib gas field and the sub-commercial Corrib North gas discovery (well 18/20-7). In other basins with similar geology, such as the East Irish Sea Basin, the presence of halite in the Upper Triassic seal overlying the Lower Triassic reservoir is considered essential for low-risk fluid containment (*e.g.* Seedhouse and Racey, 1997)

5.3. Upper Jurassic storage play (J_R)

Several kilometres of Jurassic sediments are present throughout the Slyne and Erris basins, representing the main syn-rift package in the study area. No Jurassic sediments have been encountered in the Donegal Basin to date (Fig. 5C). The Jurassic can be broadly subdivided into two sections: predominantly marine Lower and Middle Jurassic sections belonging to the Lias and Kite groups respectively, and an Upper Jurassic section consisting of terrestrial, fluvial and estuarine sediments which belong to the Beara and Muckross groups (Fig. 4). A minor regional unconformity separates these two syn-rift packages (Fig. 4).

Several reservoir-seal pairs are present throughout the Jurassic section which consist of interbedded sandstones and mudstones. Typically, the most sand-rich interval is the Upper Jurassic Minard Formation which represents the most prospective Jurassic-aged reservoir section in the study area. The Minard Formation was deposited in a predominantly terrestrial environment, with the reservoirs made up of fluvial channel-fill sandstones and overbank deposits (Merlin Energy Resources Consortium, 2020). The relative distribution of these sandstones can be observed on a root mean square (RMS) amplitude map of a 25 ms Two Way Travel Time (TWTT) window within the Minard Formation in the Central Slyne sub-basin (Fig. 7). This map shows a network of fluvial channels flowing broadly southwards towards the Porcupine Basin, as suggested by sediment provenance studies of Tyrrell *et al.* (2007). Within the Central Slyne sub-basin, channels along the margin of the basin (*i.e.* in the vicinity of the 27/5-1 well) are oriented transverse to the axis of the basin, while the channels in the centre of the basin are parallel to the basin axis, oriented broadly NNE-SSW. This map indicates that while these channelised sandstone bodies represent very high-quality reservoirs, with 20-30% porosity recorded in the core data in the 27/5-1 well (Fig. 3B; Enterprise 1996a), they are not laterally extensive, reducing the total sandstone content (*i.e.* net-to-gross) within any structural trap. This is reflected in the relatively low net-to-gross values of less than 50% observed in all wells which encounter the Minard Formation (Fig. 6C).

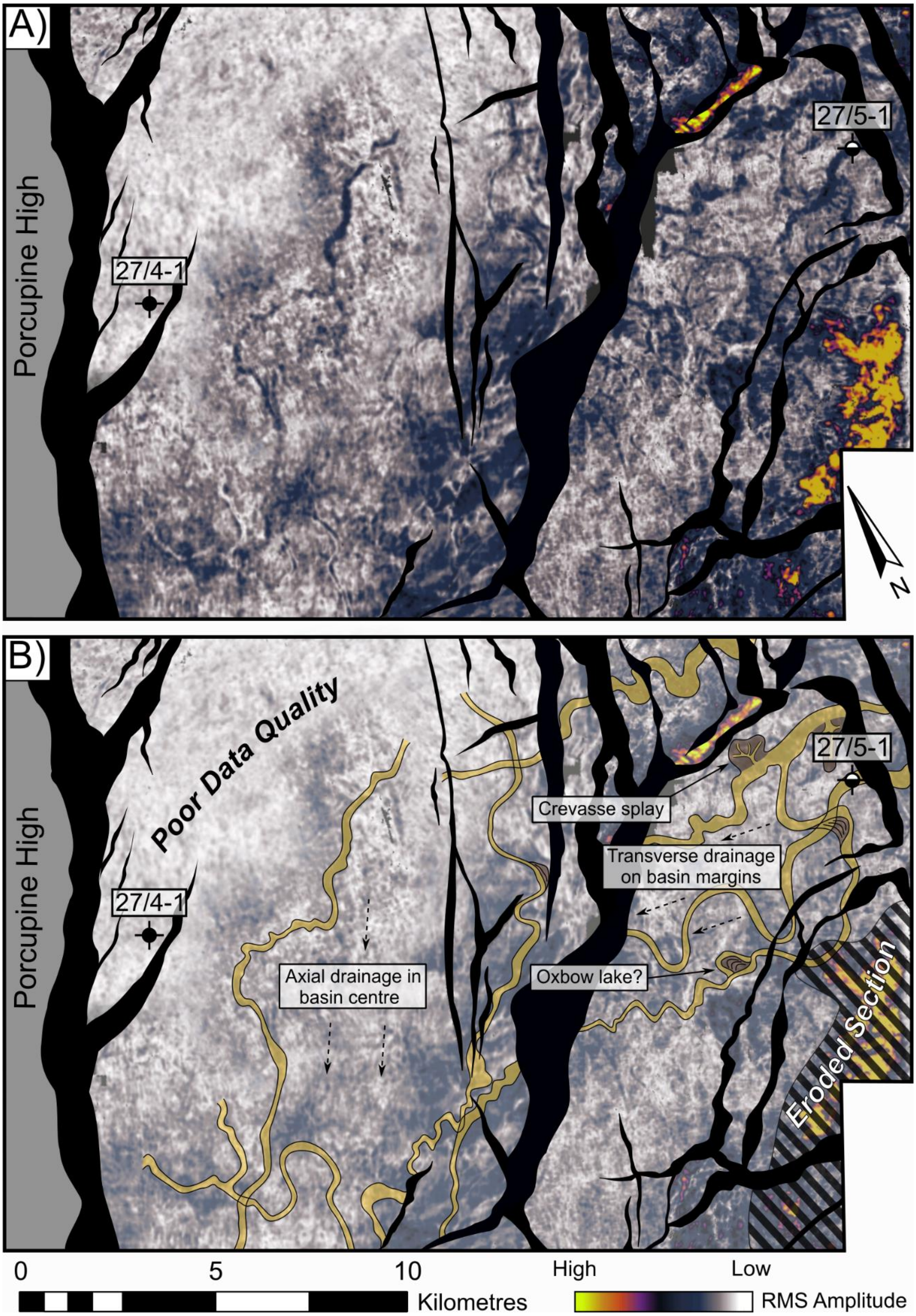

Figure 7: A) Uninterpreted and B) Interpreted RMS amplitude horizon slice in the Upper Jurassic Minard Formation from the Central Slyne sub-basin illustrating the distribution of fluvial reservoir sandstones in this storage play. Dashed arrows are used to indicate broad paleoflow directions. Fault heave at this horizon is illustrated with black polygons. See Figure 2 for map location.

The interbedded mudstones within the Minard Formation represent continental and lacustrine sediments deposited on the floodplains around the Late Jurassic river systems. These are the principal seals to the interbedded Upper Jurassic sandstones and are likely to be laterally extensive, as suggested by the RMS amplitude map in Figure 7. The integrity of these mudstones as suitable seals does warrant further investigation, as several breached hydrocarbon accumulations have been encountered in previous exploration wells (*e.g.* 18/20-1, 19/11-1A, 27/5-1 and 27/13-1A). The breaching of these paleo-accumulations is attributed to post-charge movement on faults bounding these structural traps (Spencer and MacTiernan, 2001) although a stratigraphic leak may also have occurred through connected fluvial sandbodies.

6. Storage trap types

With the storage plays in the study area established, the variety of structural trap types are now analysed. Different structural traps are observed throughout the study area, often related to the changing geology between different basins. A key factor in the structural style of individual basins on the Irish Atlantic margin is the presence of salt layers within the sedimentary section (O'Sullivan *et al.*, 2021). Where salt is present, it will act as a layer of mechanical detachment between the sub- and supra-salt sections and lead to more ductile deformation (Hudec and Jackson, 2007). Salt can also flow and form salt structures such as salt anticlines and salt rollers (Jackson and Hudec, 2017a; Jackson and Hudec, 2017b). Areas without salt will deform in a more brittle manner.

O'Sullivan *et al*. (2021) described the extents of these salt layers in the Slyne and Erris basins using regional borehole correlations and by identifying halokinetic structures on seismic reflection data. A key control on the distribution of salt within the Permian Zechstein Group is the presence of active faults creating accommodation space during salt accumulation. In contrast, the Zechstein Group is thinner and predominately composed of carbonate and clastic rocks in areas of geological quiescence during the Permian (O'Sullivan *et al.*, 2021). There is also evidence that the distribution of the Upper Triassic Uilleann Halite Member is controlled by local extension during the Early to Middle Triassic which creates accommodation space for Late Triassic salt deposition in certain parts of the Slyne and Erris basins (O'Sullivan *et al.*, 2021, O'Sullivan and Childs, 2021). Nevertheless, significant ambiguity remains to the definitive distribution of salt in the basins offshore northwest Ireland without further drilling.

6.1. Slyne Basin

The structural style of the Southern and Central Slyne sub-basins is strongly influenced by the presence of Permian salt. The most common trap types in this part of the study area are horst blocks and tilted fault blocks both above and below the Permian salt (Fig. 8). These fault-bound structures were the most common target for hydrocarbon exploration wells in this part of the study area. Of the three exploration wells drilled in the Central Slyne sub-basin, two targeted fault-bounded horsts and encountered breached oil accumulations in Upper Jurassic reservoirs (wells 27/5-1 and 27/13-1A). Both structures show evidence of post-charge movement on the bounding faults during the Cenozoic (Fig. 8B) which may have resulted in cross-fault juxtaposition of reservoir sandstones and subsequent loss of hydrocarbon accumulations. Similar movements may yet occur on these structures, caused either by pressure changes during fluid injection or by future tectonic or glacial processes, as has been observed affecting hydrocarbon accumulations in the North Sea (*e.g.* Goffey *et al.*, 2018). This places a strong emphasis on detailed fault-seal and fault-stability analysis for any candidate storage sites which rely on a fault for closure.

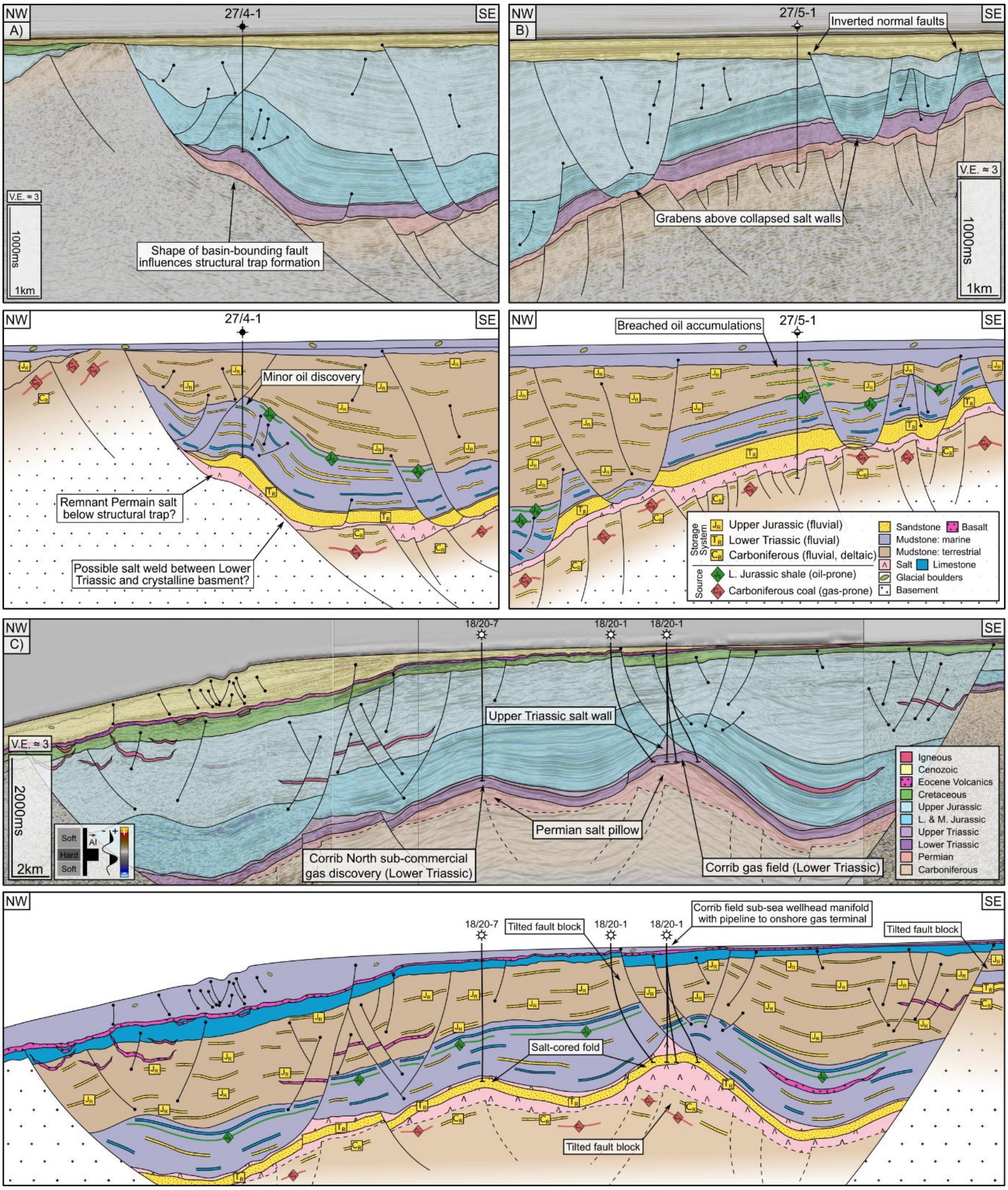

Figure 8: Schematic geoseismic sections from the Slyne Basin highlighting different structural trap types and the distribution of the key storage play components. A) Geoseismic section showing the location of the 27/4-1 'Bandon' oil discovery. B) Geoseismic section showing the impact of Cretaceous and Cenozoic fault movement on the structure hosting the 27/5-1 'Avonmore' breached oil accumulation. C) Schematic geoseismic section through the Northern Slyne sub-basin highlighting different structural trap types and the distribution of the key storage play components. Inset: A) geoseismic section showing the location of the Corrib gas field in the Lower Triassic storage play, and the breached oil accumulation in the Upper Jurassic storage play. See Figure 2 for location.

In addition to the tilted fault blocks, there are also several hanging-wall closures adjacent to the basin-bounding faults along the north-western margin of the basin (Fig. 8A). These are interpreted to have initially formed as forced folds above the incipient basin-bounding faults, before continued slip on these faults breached the folds and resulted in the current structural configuration (Dancer *et al.*, 1999; O'Sullivan *et al.*, 2021). The 27/4-1 well discovered a sub-commercial heavy oil accumulation in Lower Jurassic sandstones in one of these closures (Serica Energy, 2009), suggesting these structures are less prone to reactivation and leakage during post-rift tectonic phases than the tilted fault blocks discussed above.

The presence of two layers of salt in the Northern Slyne sub-basin (Permian and Upper Triassic, Fig. 5, 8C) results in kinematic interaction between discrete salt structures above and below the Lower Triassic section and the formation of unique structural shapes. The most common combination is a Permian salt anticline and an Upper Triassic salt roller or salt wall, with the Upper Triassic salt wall oriented parallel to the fold-axis of the Permian salt anticline. The result of these two composite salt structures are different trap types at different stratigraphic levels: the formation of the Permian salt anticline folds the overlying Lower Triassic reservoir to form a four-way dip closure sealed by the overlying Upper Triassic salt. Tilted fault blocks and horsts form in the Jurassic section above the Upper Triassic salt structures (Fig. 8C). The presence of the Upper Triassic salt in this part of the study area significantly reduces the risk of top-seal failure for fluids stored in the Lower Triassic storage play relative to other parts of the study area where the Upper Triassic section is composed primarily of red mudstone. This is proven by the presence of both the Corrib and Corrib North (18/20-7) gas accumulations in the Lower Triassic despite significant post-charge basin modification (*e.g.* Dancer *et al.*, 2005; O'Sullivan *et al.*, 2022).

6.2. Erris Basin

The Southern Erris sub-basin dips steeply towards the northwest due to thermal subsidence in the neighbouring Rockall Basin (Fig. 9A). The Southern Erris sub-basin is also the deepest part of the study area, with most of the basin located in water depths in excess of 1000 metres (Fig. 9A). Tilted fault blocks are the most common trap type in the Upper Jurassic storage play, with most bounded by westward dipping faults soling out in either the Upper Triassic or Permian salt layers (Fig. 9A). Structural traps in the Lower Triassic storage play are more varied, with some salt-cored folds like those found in the Northern Slyne sub-basin being observed, alongside fault-bound horsts encased in salt (Fig. 9A).

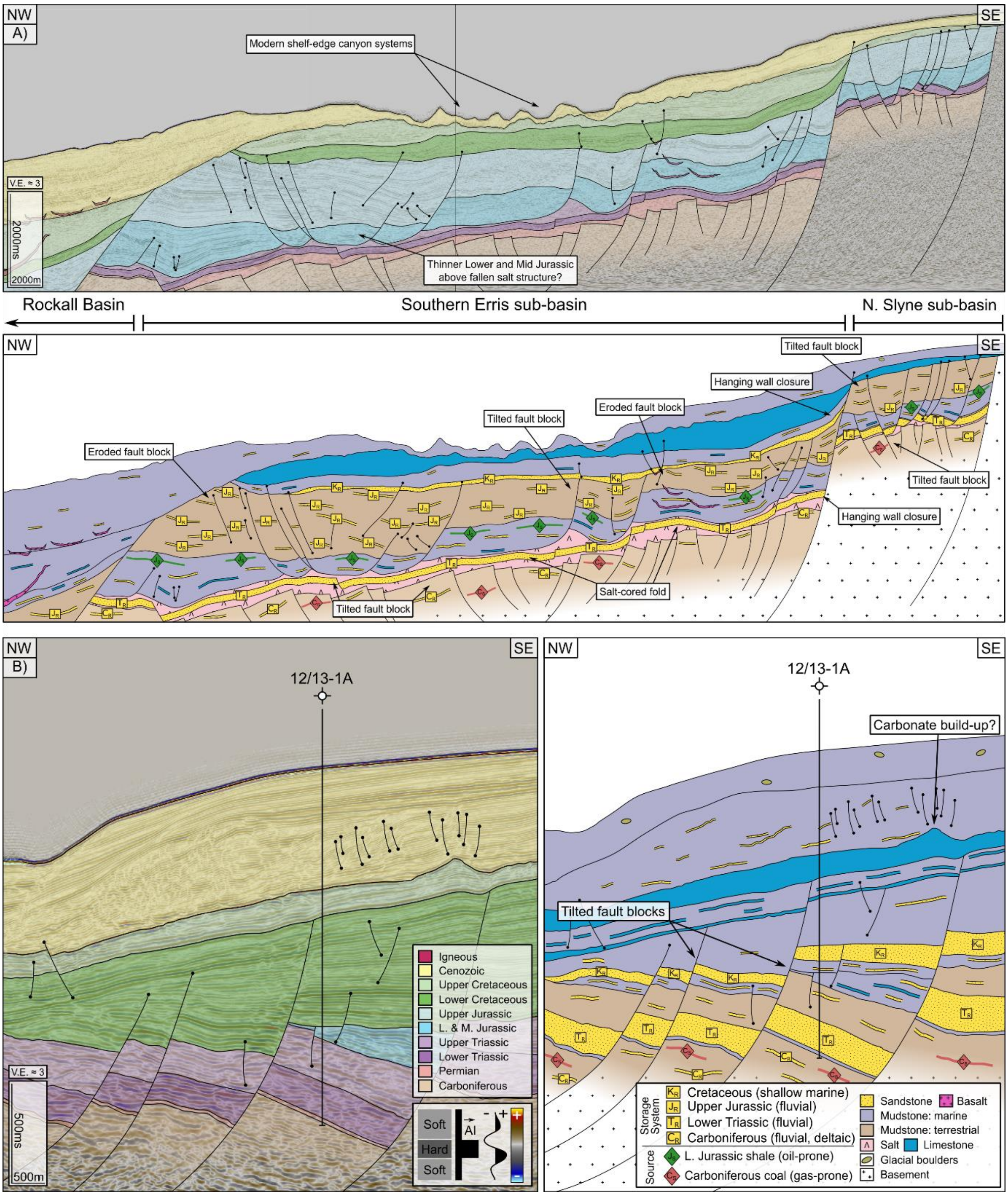

Figure 9: Schematic geoseismic sections from the Slyne Basin highlighting different structural trap types and the distribution of the key storage play components. A) Schematic geoseismic section through the Southern Erris and Northern Slyne sub-basins highlighting different structural trap types and the distribution of the key storage play components. See Figure 2 for location. B) Geoseismic section and schematic play cartoon from the Northern Erris sub-basin highlighting structural trap types and the distribution of the key storage play components. See Figure 2 for location.

The structural style in the Northern Erris sub-basin is noticeably different from the Southern Erris sub-basin due to the lack of either Permian or Upper Triassic salt layers. The basin is characterised by several north-westward-dipping tilted fault blocks covered by a thick Cretaceous and Cenozoic section (Fig. 9B). The Upper Jurassic storage play is largely absent in this part of the study area (Fig. 6C, 9B), likely due to kilometre-scale uplift and erosion during the Early Cretaceous along the flanks of the Rockall Basin (Chapman *et al.*, 1999; Corcoran and Mecklenburgh, 2005). This leaves the Lower Triassic and Carboniferous storage plays as viable reservoir units in the Northern Erris sub-basin in mostly fault-bounded structural traps (Fig. 9B).

6.3. Donegal Basin

The Donegal Basin is predominantly a Carboniferous-aged basin which formed prior to the Variscan Orogeny and was partially inverted by compressional forces associated with that mountain-building event, (Dobson and Whittington, 1992). There is no proven Permian or Mesozoic stratigraphy in either of the two wells drilled in the basin (Merlin Energy Resources Consortium, 2020), meaning that the Carboniferous storage play represents the only proven reservoir-seal pair (Fig. 5B, 5C). There is evidence on seismic sections for some Permo-Mesozoic sediment being preserved in the hangingwalls of major faults, although this remains speculation at present (Fig. 10).

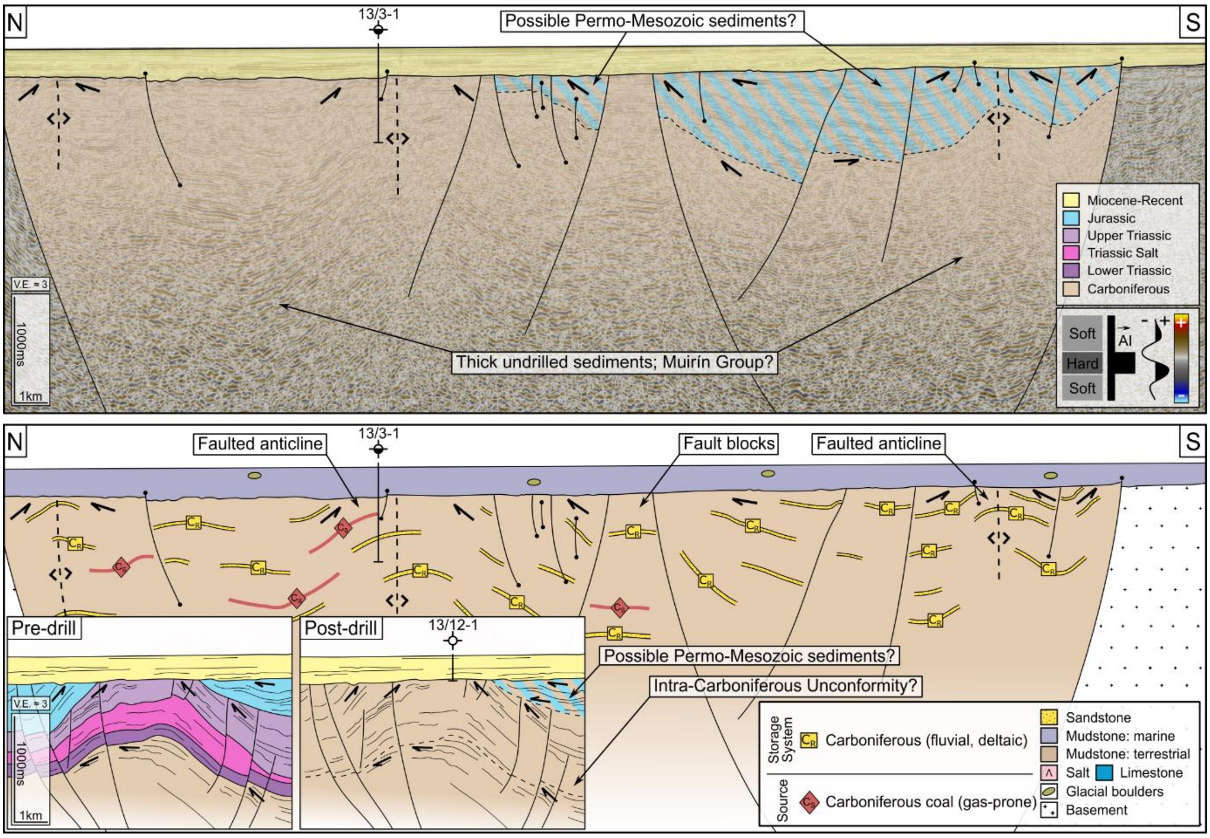

Figure 10: Geoseismic section and schematic play cartoon through the Donegal Basin highlighting different structural trap types and the distribution of the key storage play components. See Figure 2 for location. Inset: pre- and post-drill interpretation of the geology of the Inishbeg structure targeted by the 13/12-1 well showing the initial interpretation of the basin as a Mesozoic depocentre.

The basin is characterised by broad, relatively symmetrical folds with axes oriented broadly E-W, wavelengths typically between 10 and 15 km wide and amplitudes of 1-2 km (Fig. 10). The broad folds represent the primary structural trap type in the Donegal Basin which could be used for subsurface storage. They are cut by several normal faults, which may be related to regional post-Variscan extension in either the Permian, Jurassic or Cretaceous. Some of these faults are also observed offsetting the Base-Cenozoic unconformity, indicating relatively recent minor fault movement similar to the other basins in the study area. Some of these recently active faults have been linked to seafloor seepage features such as pockmarks which suggests these faults represent pathways for hydrocarbon migration to the shallow seabed and potential leak points for any fluids stored in the Carboniferous sandstone storage play. (Garcia *et al.*, 2014). Folds unaffected by the post-folding normal faulting are present in the Donegal Basin (Fig. 10) and may represent more favourable storage sites.

6.4. Review of storage plays offshore northwestern Ireland.

As previously noted, not all storage plays will be suitable hosts for either CO_2 or H_2 storage. Notable features of both the Carboniferous and Upper Jurassic storage plays are the presence of breached oil accumulations in the Upper Jurassic reservoirs of the Slyne Basin and evidence of active hydrocarbon seepage to the seabed in the Donegal Basin. These suggest the interbedded mudstones do not always provide competent seals to hydrocarbon accumulations and therefore are less attractive as subsurface storage sites for CO_2 and particularly H_2, given its very low capillary entry pressure and high diffusivity. Structural traps which have clear evidence of Cenozoic reactivation of their bounding faults maybe be prone to further fault movement and fluid leakage due to pressure changes during injection. However, the 27/4-1 'Bandon' oil accumulation does indicate some structures have acted as suitable hydrocarbon traps over geological timescales, although it is important to caveat this oil accumulation was found in a Lower Jurassic sandstone (Serica Energy, 2009). An additional concern for the Carboniferous storage play is the uncertain preservation of reasonable porosity and permeability due to its deeper burial and compaction (*e.g.* Fig. 3C). Therefore, structural traps in both the Carboniferous and Upper Jurassic plays which have not undergone later reactivation are more appealing sites for further investigation for CO_2 storage, with a preference for the Upper Jurassic storage play due to better reservoir properties.

The Lower Triassic storage play hosts two natural gas accumulations which have survived Cretaceous and Cenozoic tectonic activity (Corrib and Corrib North), with the Upper Triassic salt seal playing a key part in this preservation. This salt seal will be particularly important for H_2 storage where it is present in the Northern Slyne and Southern Erris sub-basins. Neither intact nor breached hydrocarbon accumulations have been encountered in the Lower Triassic reservoir where the Upper Triassic seal is predominately mudstone so less is known about how competent these rocks would be as a seal. Research from the East Irish Sea Basin, which hosts several large oil and gas fields in an equivalent Triassic reservoir-seal pair to that found in the Slyne and Erris basins, and other basins in the Irish Sea shows that salt seals have proven crucial in preserving subsurface fluid accumulations during post-glacial rebound and trap modification (*e.g.* Seedhouse and Racey, 1997; Duncan *et al.*, 1998; Naylor and Shannon, 1999). The Lower Triassic reservoir also has notably higher porosity and net-to-gross than both the Upper Jurassic and Carboniferous reservoirs in the limited dataset available in these basins (Fig. 3, 6). The Lower Triassic storage play also benefits from the significant reservoir characterisation that has taken place at the Corrib gas field, where key parameters like vertical and horizontal permeability and static and dynamic pressure regimes alongside reservoir connectivity can be used as an analogue for the Lower Triassic reservoir throughout the study area. Therefore, the Lower Triassic storage play is likely the most suitable of the three plays analysed in this study for further investigation, particularly where it is overlain by a salt seal.

7. Example storage site case studies

With the methodology established and the geology of study area characterised, three potential storage sites are investigated. Each site has different amounts of data available and is outlined in detail below:

- The Corrib structure is covered by several vintages of 3D seismic data including a high-quality ocean-bottom cable survey. This is tied to data from eight wells. Structural closures are mapped in the Upper Jurassic and Lower Triassic storage plays.
- The Inishmore structure is covered by reasonable quality 3D seismic data. The nearest exploration well (27/13-1A) is located 25 kilometres to the north of the structure but only provides geological control down to the Lower Jurassic. The nearest well which penetrates the Triassic and Carboniferous (27/5-1) is located 65 kilometres to the north of the Inishmore structure. Structural closures are mapped in the Upper Jurassic, Lower Triassic, and Carboniferous storage plays.
- The Inishbeg structure is covered by a grid of 2D seismic reflection lines with a one-five kilometre spacing. A very shallow exploration well (13/12-1) penetrated the upper 112 metres of Carboniferous rocks beneath Base Cenozoic Unconformity. The nearest exploration wells of significance (13/3-1 and 12/13-1A) are 35 and 45 kilometres to the north and west of the Inishbeg structure respectively. A structural closure is mapped in the Carboniferous storage play.

7.1. Corrib

The Corrib structure hosts the eponymous Corrib gas field in the Northern Slyne Basin. The field was discovered in 1996 with the 18/20-1 well, which encountered breached oil accumulations in the Jurassic tilted fault block followed by the gas accumulation in the Corrib Sandstone Formation (Enterprise, 1996b). The original gas in place in the field was estimated to be 1.2 trillion cubic feet, with recoverable reserves of approximately 870 billion cubic feet (Dancer *et al.*, 2005).

Three principal components comprise the structure; a Permian salt anticline folds the overlying Lower Triassic and forms a four-way dip-closure (Fig. 11). This is overlain by a narrow Upper Triassic salt wall broadly parallel to the fold axis of the Permian salt anticline (Fig. 11). The Jurassic overburden is deformed by a series of faults related to the growth of the salt structures, with the largest being the Corrib Fault (O'Sullivan and Childs, 2021), which dips towards the southeast (Fig. 11). The footwall of this fault forms a tilted fault block structural closure. A relatively thin veneer of unconformable Cretaceous and Cenozoic sediments records the complex post-rift evolution of the area (Dancer *et al.*, 2005; O'Sullivan and Childs, 2021).

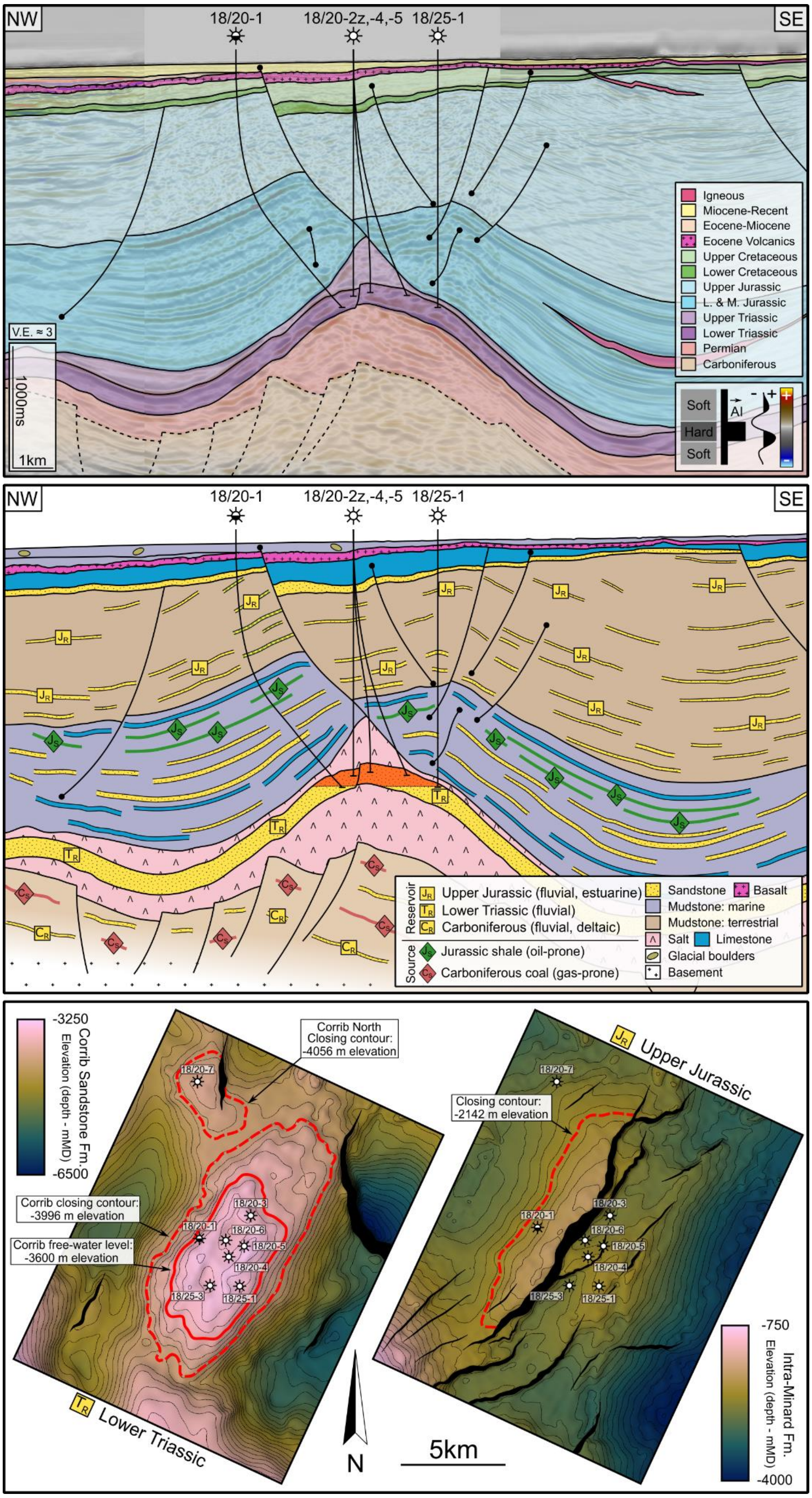

Figure 11: Overview of the Corrib structure. A) Geoseismic section through the Corrib structure. B) Schematic cross-section showing the various storage plays present in the Corrib structure. C) Intra-Upper Jurassic structure map showing the closures mapped in the Upper Jurassic storage play. D) Top Lower Triassic structure map showing the closure mapped in the Lower Triassic storage play. See Figure 2 for map location.

Two storage plays are evaluated at Corrib: The Lower Triassic storage play, which currently hosts the gas accumulation in the anticlinal closure, and the Upper Jurassic storage play, which contains evidence of a paleo-oil accumulation which has been destroyed, likely by post-charge movement on the fault bounding the tilted block (Enterprise, 1996b). The Carboniferous storage play is not well imaged on available seismic and is likely to be buried too deeply (over five kilometres present-day) to preserve meaningful reservoir quality. Two spill points were used for the Lower Triassic storage play at Corrib given existing information: the first being located at 3600 mTVDSS matching the gas-water contact which was first encountered during the discovery of the field, and the second at 3996 mTVDSS representing the spill point of the total structural closure. Previous authors have provided several possible explanations for the underfilled nature of the Corrib structure, including a sub-seismic leaking fault or salt weld (Corcoran and Mecklenburgh, 2005) or post-charge modification of the structure (O'Sullivan *et al.*, 2021). In addition to the main Corrib closure, the storage volume of the satellite gas accumulation discovered in the Corrib North structure was also modelled, although it should be noted that the reservoir quality of the Triassic was found to be significantly poorer than prognosed (Fig. 3A, 11; Shell, 2011).

Table 2: Inputs and results for storage assessment in the Corrib and Corrib North structures.

<table>
<tr><th>Structure</th><th colspan="6">Corrib Jurassic</th><th colspan="6">Corrib Triassic (Gas)</th><th colspan="6">Corrib Triassic (Full Closure)</th><th colspan="6">Corrib North</th></tr>
<tr><td>Water depth (m)</td><td colspan="18">355</td><td colspan="6">401</td></tr>
<tr><td>Top reservoir depth (mTVDSS)</td><td colspan="6">1724</td><td colspan="6">3231</td><td colspan="6">3231</td><td colspan="6">3839</td></tr>
<tr><td>Base closure depth (mTVDSS)</td><td colspan="6">2142</td><td colspan="6">3600</td><td colspan="6">3996</td><td colspan="6">4056</td></tr>
<tr><td>Structural relief (m)</td><td colspan="6">417</td><td colspan="6">369</td><td colspan="6">765</td><td colspan="6">217</td></tr>
<tr><td>Volumetric Input</td><td colspan="3">Maximum</td><td colspan="3">Minimum</td><td colspan="3">Maximum</td><td colspan="3">Minimum</td><td colspan="3">Maximum</td><td colspan="3">Minimum</td><td colspan="3">Maximum</td><td colspan="3">Minimum</td></tr>
<tr><td>GRV (m3)</td><td colspan="3">4.75E+09</td><td colspan="3">3.81E+09</td><td colspan="3">4.61E+09</td><td colspan="3">3.69E+09</td><td colspan="3">1.81E+10</td><td colspan="3">1.45E+10</td><td colspan="3">8.18E+08</td><td colspan="3">6.56E+08</td></tr>
<tr><td>Porosity (%)</td><td colspan="3">31</td><td colspan="3">1</td><td colspan="3">15</td><td colspan="3">1</td><td colspan="3">15</td><td colspan="3">1</td><td colspan="3">13</td><td colspan="3">1</td></tr>
<tr><td>Net-to-gross (%)</td><td colspan="3">46</td><td colspan="3">11</td><td colspan="3">87</td><td colspan="3">48</td><td colspan="3">87</td><td colspan="3">48</td><td colspan="3">87</td><td colspan="3">48</td></tr>
<tr><td>Fluid saturation (%)</td><td colspan="3">65</td><td colspan="3">20</td><td colspan="3">65</td><td colspan="3">20</td><td colspan="3">65</td><td colspan="3">20</td><td colspan="3">65</td><td colspan="3">20</td></tr>
<tr><td>CO_2 Density (kg/m^3)</td><td colspan="3">715</td><td colspan="3">703</td><td colspan="3">685</td><td colspan="3">681</td><td colspan="3">685</td><td colspan="3">679</td><td colspan="3">679</td><td colspan="3">677</td></tr>
<tr><td>H_2 Density (kg/m^3)</td><td colspan="3">14.9</td><td colspan="3">12.5</td><td colspan="3">22.4</td><td colspan="3">20.6</td><td colspan="3">23.7</td><td colspan="3">20.6</td><td colspan="3">24.6</td><td colspan="3">23.3</td></tr>
<tr><td>Volumetric Results</td><td colspan="2">P10</td><td colspan="2">P50</td><td colspan="2">P90</td><td colspan="2">P10</td><td colspan="2">P50</td><td colspan="2">P90</td><td colspan="2">P10</td><td colspan="2">P50</td><td colspan="2">P90</td><td colspan="2">P10</td><td colspan="2">P50</td><td colspan="2">P90</td></tr>
<tr><td>CO_2 (Million Tonnes)</td><td colspan="2">136</td><td colspan="2">48</td><td colspan="2">11</td><td colspan="2">119</td><td colspan="2">54</td><td colspan="2">15</td><td colspan="2">497</td><td colspan="2">232</td><td colspan="2">62</td><td colspan="2">14</td><td colspan="2">6</td><td colspan="2">2</td></tr>
<tr><td>H_2 (TWh)</td><td colspan="2">48</td><td colspan="2">17</td><td colspan="2">5</td><td colspan="2">79</td><td colspan="2">32</td><td colspan="2">9</td><td colspan="2">308</td><td colspan="2">147</td><td colspan="2">39</td><td colspan="2">13</td><td colspan="2">6</td><td colspan="2">2</td></tr>
</table>

It should be noted that the calculations presented above do not account for residual hydrocarbon accumulations. This includes both the residual gas in the Lower Triassic reservoir and the paleo-oil accumulation encountered in the Upper Jurassic reservoir. Modelling has indicated that residual gas can impact the injectivity, density and plume size of CO_2 injected into old gas fields (*e.g.* Oldenburg and Doughty, 2011). While this is not considered in the methodology presented in this study, residual gas accumulations will need to be accounted for in more detailed, site-specific investigations and modelling.

7.2. Inishmore

The Inishmore structure is located in the centre of the Southern Slyne sub-basin and consists of a tilted fault block above a large salt roller of Permian salt, oriented NE-SW with the main fault bounding the structure along its south-eastern margin (Fig. 12). The structure has a prominent angular unconformity along its crest at the base of the Upper Jurassic section, indicating that the salt roller had already formed during the Early to Middle Jurassic, likely due to regional extension, before further salt movement and growth during the Late Jurassic

(O'Sullivan *et al.*, 2021). Unlike other structures which have undergone post-rift modification such as the horst block drilled by the 27/5-1 well (Fig. 8B), the faults bounding the Inishmore structure do not offset the Base Cenozoic Unconformity (Fig. 12), suggesting they may not have been reactivated during the Cenozoic. However, the lack of any Cretaceous sediments to record fault movement during the Cretaceous does not preclude any post-rift movement on the bounding faults (*e.g.* O'Sullivan *et al.*, 2022).

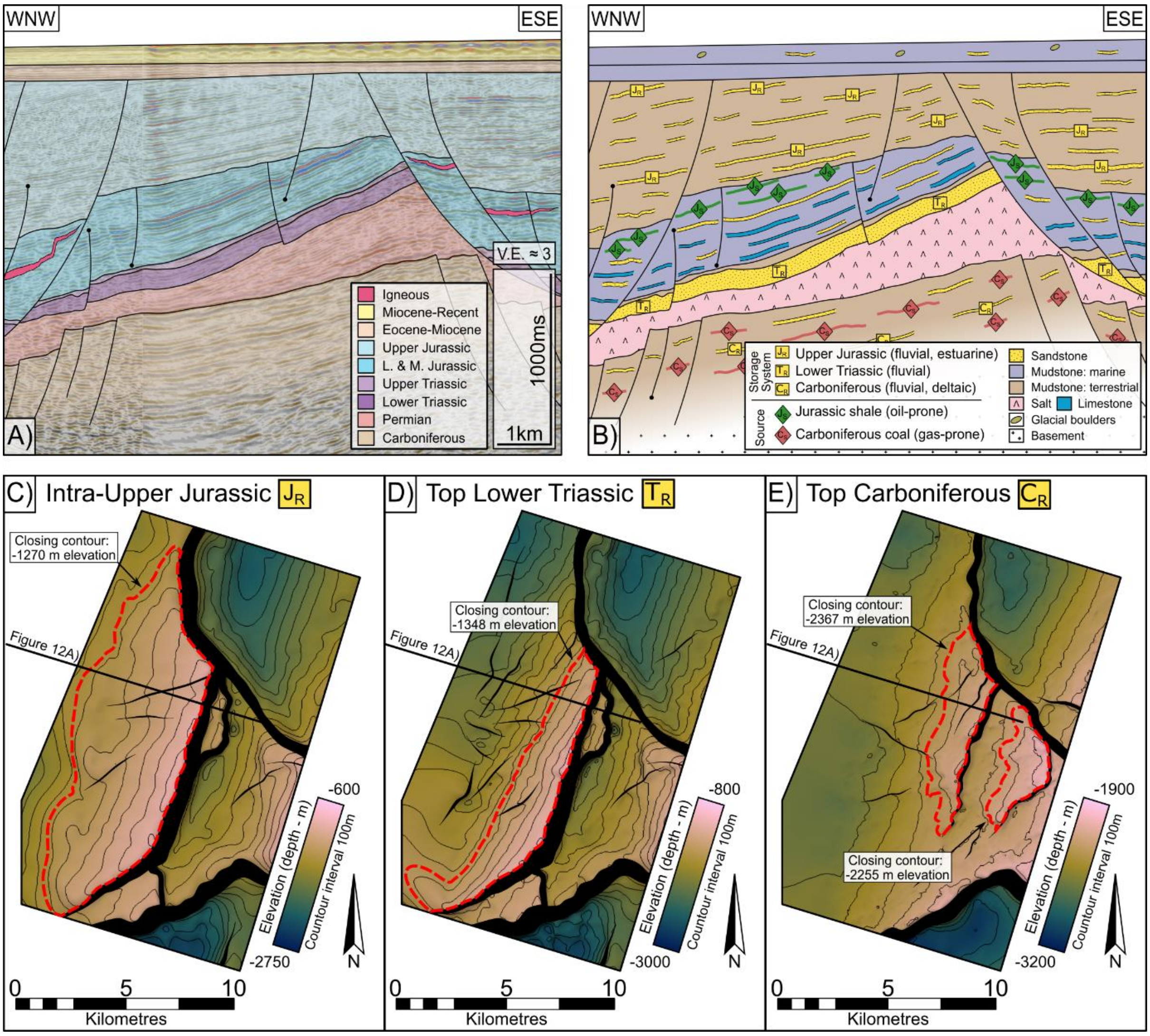

Figure 12: Overview of the Inishmore structure. A) Geoseismic section through the Inishmore structure. B) Schematic cross-section showing the various storage plays present in the Inishmore structure. C) Intra-Upper Jurassic structure map showing the closure mapped in the Upper Jurassic storage play. D) Top Lower Triassic structure map showing the closure mapped in the Lower Triassic storage play. E) Top Carboniferous structure map showing the closures mapped in the Carboniferous storage play. See Figure 2 for map location.

Stacked structural traps are mapped in each storage play in the Inishmore structure; two large closures in the Upper Jurassic and Lower Triassic storage plays are observed bounded by the main fault which soles out in the Permian salt, while two smaller closures are observed in the Carboniferous storage play (Fig. 12C-E). The Upper Jurassic reservoir is shallower than the 800 metres depth requirement for CO_2 storage but is deep enough for H_2 storage (Fig. 12C), while both the Triassic and Carboniferous reservoirs are deep enough to be effective for both

H_2 and CO_2 storage (Fig. 12D, E). The range of fluid volumes for each storage play are presented in Table 3.

Table 3: Inputs and results for storage assessment in the Inishmore structure.

<table>
<tr><th>Structure</th><th colspan="6">Inishmore Jurassic</th><th colspan="6">Inishmore Triassic</th><th colspan="6">Inishmore Carboniferous 1</th><th colspan="6">Inishmore Carboniferous 2</th></tr>
<tr><td>Water depth (m)</td><td colspan="24">151</td></tr>
<tr><td>Top reservoir depth (mTVDSS)</td><td colspan="6">657</td><td colspan="6">818</td><td colspan="6">2031</td><td colspan="6">2177</td></tr>
<tr><td>Base closure depth (mTVDSS)</td><td colspan="6">1270</td><td colspan="6">1348</td><td colspan="6">2255</td><td colspan="6">2367</td></tr>
<tr><td>Structural relief (m)</td><td colspan="6">613</td><td colspan="6">530</td><td colspan="6">224</td><td colspan="6">190</td></tr>
<tr><th>Volumetric Input</th><th colspan="3">Maximum</th><th colspan="3">Minimum</th><th colspan="3">Maximum</th><th colspan="3">Minimum</th><th colspan="3">Maximum</th><th colspan="3">Minimum</th><th colspan="3">Maximum</th><th colspan="3">Minimum</th></tr>
<tr><td>GRV (m3)</td><td colspan="3">1.68E+10</td><td colspan="3">1.35E+10</td><td colspan="3">5.66E+09</td><td colspan="3">4.54E+09</td><td colspan="3">6.91E+08</td><td colspan="3">5.54E+08</td><td colspan="3">1.25E+09</td><td colspan="3">9.99E+08</td></tr>
<tr><td>Porosity (%)</td><td colspan="3">39</td><td colspan="3">4</td><td colspan="3">29</td><td colspan="3">9</td><td colspan="3">20</td><td colspan="3">1</td><td colspan="3">19</td><td colspan="3">1</td></tr>
<tr><td>Net-to-gross (%)</td><td colspan="3">46</td><td colspan="3">11</td><td colspan="3">87</td><td colspan="3">48</td><td colspan="3">71</td><td colspan="3">11</td><td colspan="3">71</td><td colspan="3">11</td></tr>
<tr><td>Fluid saturation (%)</td><td colspan="3">65</td><td colspan="3">20</td><td colspan="3">65</td><td colspan="3">20</td><td colspan="3">65</td><td colspan="3">20</td><td colspan="3">65</td><td colspan="3">20</td></tr>
<tr><td>CO_2 Density (kg/m^3)</td><td colspan="3">N/A</td><td colspan="3">N/A</td><td colspan="3">770</td><td colspan="3">733</td><td colspan="3">706</td><td colspan="3">699</td><td colspan="3">703</td><td colspan="3">697</td></tr>
<tr><td>H_2 Density (kg/m^3)</td><td colspan="3">9.9</td><td colspan="3">4.9</td><td colspan="3">10.6</td><td colspan="3">6.4</td><td colspan="3">16.1</td><td colspan="3">14.3</td><td colspan="3">16.9</td><td colspan="3">15.5</td></tr>
<tr><th>Volumetric Results</th><th colspan="2">P10</th><th colspan="2">P50</th><th colspan="2">P90</th><th colspan="2">P10</th><th colspan="2">P50</th><th colspan="2">P90</th><th colspan="2">P10</th><th colspan="2">P50</th><th colspan="2">P90</th><th colspan="2">P10</th><th colspan="2">P50</th><th colspan="2">P90</th></tr>
<tr><td>CO_2 (Million Tonnes)</td><td colspan="2">N/A</td><td colspan="2">N/A</td><td colspan="2">N/A</td><td colspan="2">310</td><td colspan="2">174</td><td colspan="2">92</td><td colspan="2">16</td><td colspan="2">7</td><td colspan="2">2</td><td colspan="2">29</td><td colspan="2">11</td><td colspan="2">3</td></tr>
<tr><td>H_2 (TWh)</td><td colspan="2">125</td><td colspan="2">47</td><td colspan="2">16</td><td colspan="2">84</td><td colspan="2">45</td><td colspan="2">24</td><td colspan="2">8</td><td colspan="2">2</td><td colspan="2">1</td><td colspan="2">13</td><td colspan="2">4</td><td colspan="2">1</td></tr>
</table>

The influence of salt tectonics on storage volumes can be readily observed in the Inishmore structure; the two phases of fault movement and salt roller growth which affected the Triassic reservoir have resulted in a more steeply dipping top reservoir surface and a smaller closure area (Fig. 12) and smaller storage volume (Table 3) while the overlying Upper Jurassic reservoir has only undergone one episode of tilting during the regional extension in the Late Jurassic, resulting in a shallower dip and greater closure volume.

7.3. Inishbeg

The Inishbeg structure is an anticline located on the southern margin of the Donegal Basin (Fig. 2A). It was previously a hydrocarbon exploration target, with a prognosed Mesozoic section forming a similar structural trap as the Corrib gas field (Fig. 10 inset). The structure was partially tested in 2006 with the 13/12-1 well, which was terminated after only seven days of drilling when it was confirmed that the Mesozoic section was absent and Carboniferous sediments were present directly beneath the Base-Cenozoic Unconformity (Lundin, 2006). Nevertheless, the well only penetrated the upper 100 metres of the Carboniferous section, and the four-way dip closure imaged on seismic data was not fully tested. This same structure is assessed here for its subsurface storage potential and showcases the potential of the Carboniferous storage play in the Donegal Basin (Fig. 13).

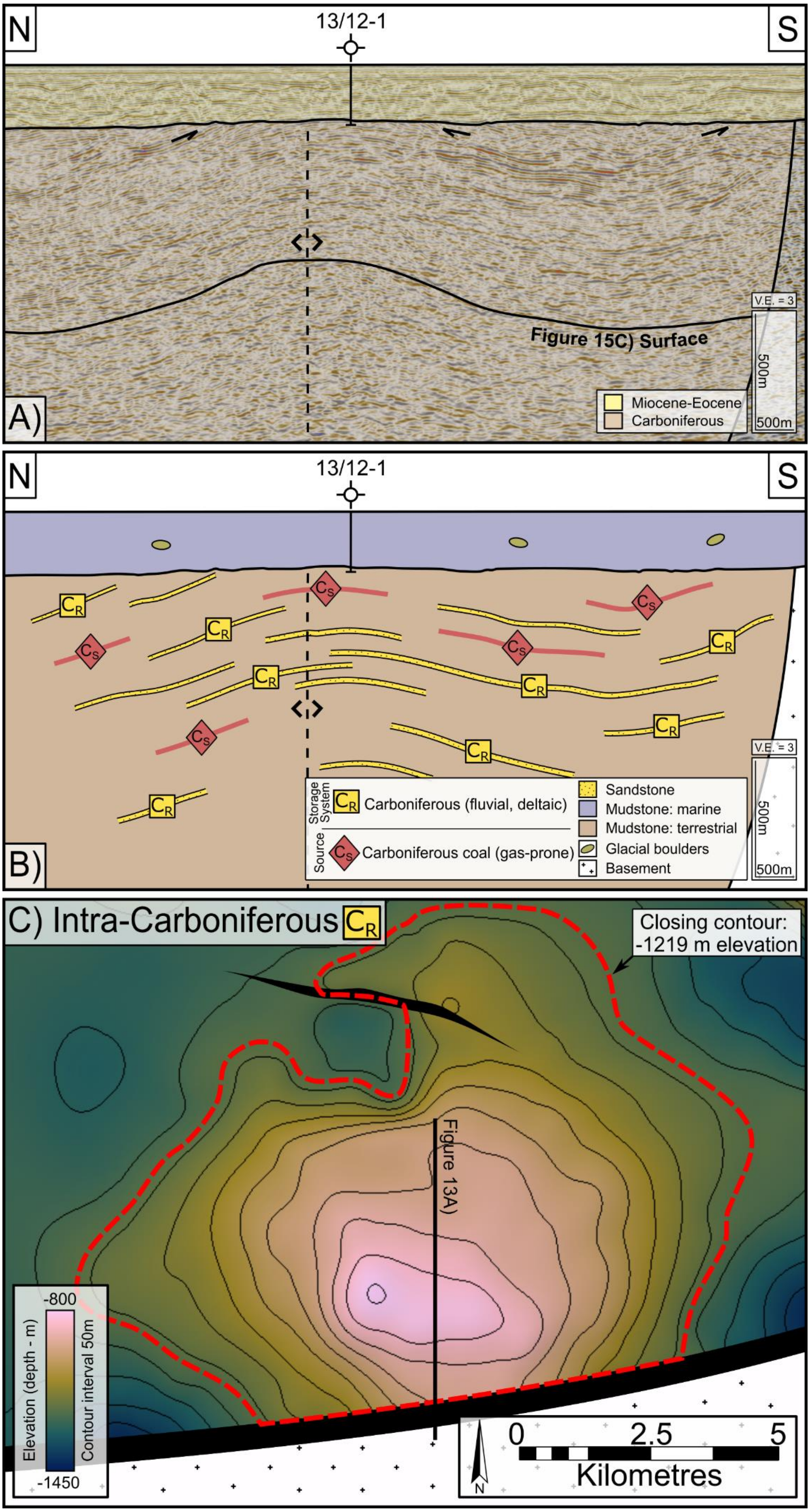
N
13/12-1
S
Figure 15C) Surface
V.E. = 3
500m
500m
Miocene-Eocene
Carboniferous
A)
N
13/12-1
S
V.E. = 3
500m
500m
Storage System
Carboniferous (fluvial, deltaic)
Source
Carboniferous coal (gas-prone)
Sandstone
Mudstone: marine
Mudstone: terrestrial
Glacial boulders
Basement
B)
C) Intra-Carboniferous
Closing contour:
-1219 m elevation
Figure 13A)
-800
Elevation (depth - m)
Contour interval 50m
-1450
0
2.5
5
Kilometres
N

Figure 13: Overview of the Inishbeg structure. A) Geoseismic section through the Inishbeg structure. B) Schematic cross-section showing the Carboniferous storage play present in the Inishbeg structure. C) Intra-Carboniferous structure map showing the closure mapped in the Carboniferous storage play. See Figure 2 for map location.

As the seismic character of the Carboniferous section is relatively homogeneous and lacks distinct seismic markers, a representative reservoir surface was mapped with a structural high at 800m depth (Fig. 13). This reflector was chosen to give a reasonable volumetric estimate considering the typical depth of around 800m where CO_2 enters a supercritical state. The trap is partially closed by a major fault which forms the southern boundary of the Donegal Basin (Fig. 13). Along-strike this fault has been reactivated during the Cenozoic with a reverse sense of motion (Fig. 10) which emphasises the importance of detailed fault analysis in further investigation of these structures.

Table 4: Inputs and results for storage assessment in the Inishbeg structure.

Structure	Inishbeg Carboniferous		
Water depth (m)	97		
Top reservoir depth (mTVDSS)	800		
Base closure depth (mTVDSS)	1219		
Structural relief (m)	419		
Volumetric Input	**Maximum**		**Minimum**
GRV (m3)	1.41E+10		1.13E+10
Porosity (%)	33		3
Net-to-gross (%)	71		11
Fluid saturation (%)	65		20
CO_2 Density (kg/m^3)	770		739
H_2 Density (kg/m^3)	9.3		6.4
Volumetric Results	**P10**	**P50**	**P90**
CO_2 (Million Tonnes)	566	242	60
H_2 (TWh)	140	50	12

As previously stated, these values represent theoretical storage volumes, with effective storage volumes for CO_2 expected to be at least an order of magnitude smaller when the storage efficiency factor and the regional aquifer volume and seal capacity is considered. Nevertheless, given only three structural traps have considered, this demonstrates the considerable storage potential in Ireland's sedimentary basins across the various structural traps. For reference, Ireland has annual emissions of 61.8 million tonnes CO_2 equivalent *sensu* SEAI, 2022 and monthly energy demands of between 2.5 to 3.2 TWh (SEAI, 2022).

8. Discussion

8.1. Other potential storage plays on the Irish Atlantic margin

There are several other storage plays that have been previously proposed as potential exploration targets during the search for hydrocarbon resources offshore Ireland. Both Amoco (1979) and the Petroleum Affairs Division (2005) noted the presence of high-quality reservoirs in the Scatálá and Siorc Sandstone Members at the base of the Lower Cretaceous Valhall Formation in the 12/13-1A well (Fig. 11), with log-derived porosities of 15-25% recorded (Amoco, 1979). The mudstones and marls of the surrounding Valhall Formation were inferred to seal these Cretaceous sandstone reservoirs. No indications of hydrocarbons were recorded in either sandstone member (Amoco, 1979). As this reservoir-seal pair has only been encountered in a single well in the study area, it is difficult to evaluate it further.

A second potential storage play in the study area is a fractured basement reservoir along the crest of the Erris Ridge (Fig. 14) similar to that proven on the Rona Ridge in the West of Shetland region (*e.g.* Holdsworth *et al.*, 2019). This would have consisted of a reservoir where porosity was provided primarily by fracture networks in the crystalline basement of the Erris Ridge, sealed by overlying Mesozoic mudstones. Howard *et al.* (2009) mentioned that an exploration well was planned to test this reservoir in 2010 but it was ultimately never drilled. At present too little data has been acquired to adequately assess either of these two storage plays and their potential utility as part of the storage portfolio for Ireland’s energy future.

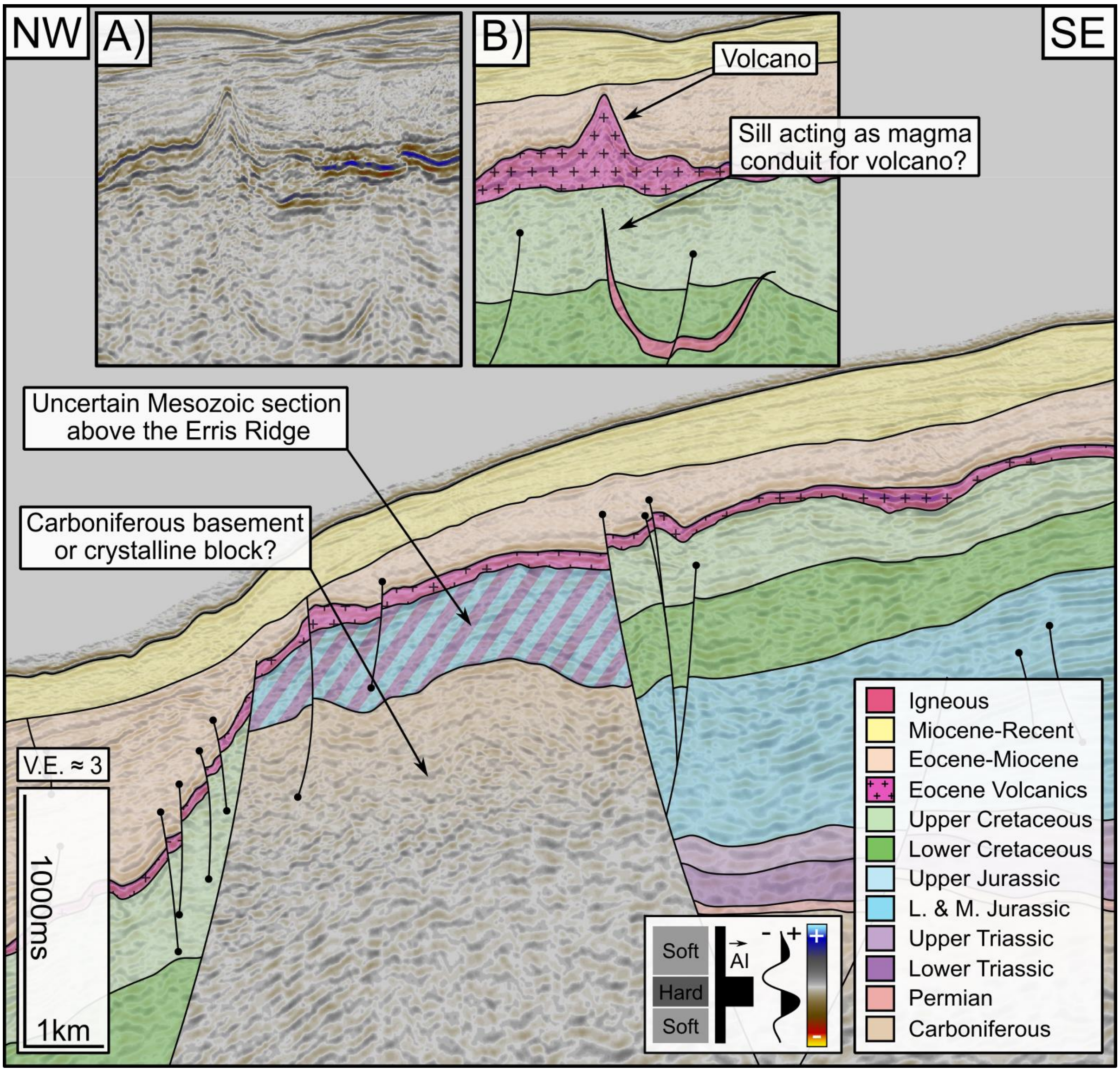

Figure 14: Geoseismic section through the Erris Ridge in the Northern Erris sub-basin. A) Uninterpreted and B) Interpreted seismic section through a volcano, demonstrating the extrusion of the Eocene lavas and the possible link with underlying igneous intrusions. See Figure 2 for map location.

8.2. Salt cavern storage on the Irish Atlantic margin

In addition to storage in porous sandstone reservoirs, artificial caverns in salt layers are commonly used across the world to store fluids in the subsurface (Casacão *et al.*, 2023; Ozarslan, 2012; Duffy *et al.*, 2022; Ramos *et al.*, 2022). The Zechstein Group within the Slyne

Basin consists of relatively clean halite and anhydrite with few interbedded insoluble sediments, with less than 2% and 6% insoluble material in the 27/5-1 and 18/25-2 wells respectively (Fig. 15). Conversely, the Uilleann Halite Member is interbedded with multiple layers of red mudstone with 12-13% insoluble material recorded in the 18/20-1 and 18/20-4 wells, although these are concentrated towards the top of the unit, with cleaner halite towards the base (Fig. 15). While not encountered in the few wells drilled offshore northwestern Ireland, igneous intrusions could also present challenges to salt cavern development, given the significant amount encountered in these basins (e.g Fig. 8C, 9A, 14). Fractured igneous intrusions could provide a pathway for fluids from storage reservoirs up to shallower layers (Fig. 15). Impurities within these salt layers would result in a sump pile at the base of any cavern, reducing the final available volume (Fig. 15). These interbedded layers of insoluble strata also represent zones of potential failure and leakage along the cavern walls (Bérest *et al.*, 2019; Duffy *et al.*, 2022). The regional extent and composition of these salt layers is reasonably well constrained using borehole and seismic reflection data, although significantly more boreholes would need to be drilled to accurately characterise salt regionally in these basins (Fig. 15; O'Sullivan *et al.*, 2021).

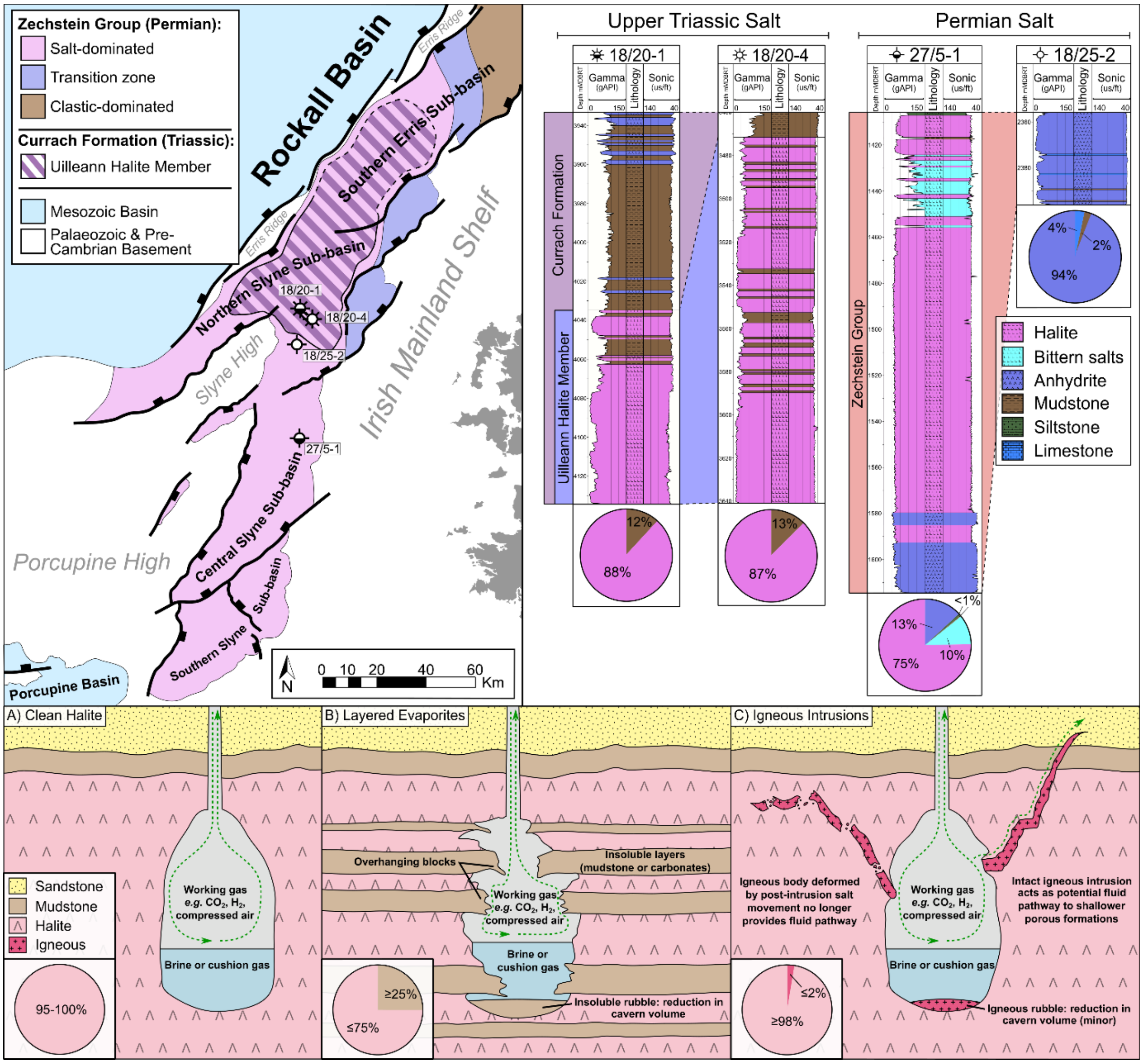

Figure 15: Map showing the distribution of Permian and Triassic salt within the Slyne and Erris basins alongside well sections comparing the composition of the Zechstein Group and the Uilleann Halite

Member, and schematic cross-sections of salt caverns in different geological settings. Map adapted from O'Sullivan et al. (2021). Note on the wells displayed in the well correlation are shown on the map. See O'Sullivan et al. (2021) for complete well correlations in both Permian and Triassic salt layers. A) Salt cavern in clean halite. B) Salt cavern in halite with interbedded insoluble mudstone layers. C) Salt cavern in halite intruded by igneous sills.

8.3. Comparison with other basins

As reference has been made to the basins offshore southern and eastern Ireland, for completeness, a brief comparison is made here with the Slyne, Erris and Donegal basins of the Irish Atlantic margin. These basins include the North and South Celtic Sea basins, the Fastnet Basin, the Central Irish Sea Basin and the Kish Bank Basin. These basins have undergone a multiphase geological evolution, including Mesozoic rifting alongside basin inversion and exhumation during the Cretaceous and Cenozoic, in a similar manner to those offshore northwest Ireland. They contain a sedimentary succession up to nine kilometres thick ranging from Permian to Cenozoic in age and which unconformably overlies a basement of Devonian to Carboniferous age (Rodriguez-Salgado *et al.*, 2020; Rowell, 1995; Shannon, 1991).

The Lower Triassic and Upper Jurassic storage plays discussed previously are common to both the Irish Atlantic margin and Celtic Sea basins including the Fastnet Basin. Additionally, the limestones and sandstones of the Middle Jurassic and sandstones of the Lower Cretaceous represent additional reservoirs, which are sealed by interbedded mudstones and the overlying Upper Cretaceous chalky limestone, representing candidate Middle Jurassic and Lower Cretaceous storage plays respectively. The Middle Jurassic is largely absent from the Fastnet Basin but the Lower Triassic, Lower Jurassic, and Lower Cretaceous are proven reservoirs in this basin (Merlin Energy Resources Consortium, 2020). In both the Central Irish Sea and Kish Bank basins, exhumation and erosion during the Cenozoic has removed any Cretaceous sediments (including any viable reservoirs) and only a thin veneer of Cenozoic sediments is present (Holford *et al.*, 2005, Murdoch *et al.*, 1995). Several other plays are present, including the Lower Triassic, Middle Jurassic and Upper Jurassic plays discussed previously.

The multitude of storage plays present in these basins are complemented by a variety of structural trap types including four-way dip closures, tilted fault blocks and salt-related folds (Fig. 16). Four-way dip closures are the most common trap type in the in Celtic Sea basins (excluding the Fastnet Basin) but are very uncommon in the Central Irish Sea and Kish Bank Basin. These structures formed in the hangingwalls of low-angle faults due to folding and reverse fault reactivation during the middle Eocene (Rodriguez-Salgado *et al.*, 2020). These structures host three now-decommissioned gas fields (Kinsale, Ballycotton and Seven Heads, Fig. 16A) which had a total production of almost 1.9 trillion cubic feet of natural gas, and also several undeveloped gas accumulations (*e.g.* Galley Head, Schull, Carrigaline and Old Head), hosted primarily hosted in the Lower Cretaceous storage play. A recent study by Rodriguez-Salgado *et al.* (2022a) has estimated a capacity of 17611 Mt CO_2 in these four-way dip-closed structures in the Celtic Sea basins.

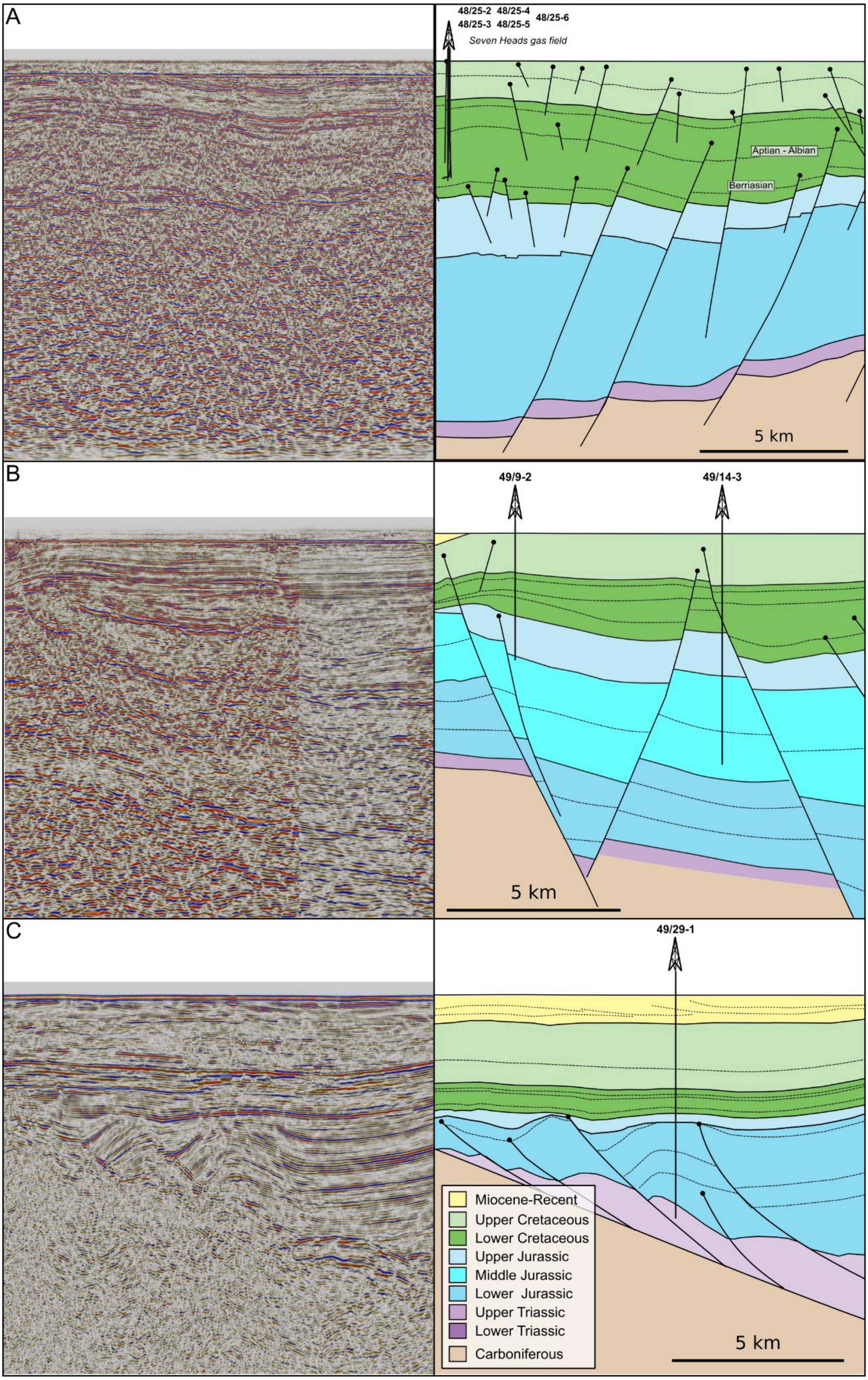

A
48/25-2 48/25-4
48/25-3 48/25-5
48/25-6
Seven Heads gas field
Aptian - Albian
Berriasian
5 km
B
49/9-2
49/14-3
5 km
C
49/29-1
Miocene-Recent
Upper Cretaceous
Lower Cretaceous
Upper Jurassic
Middle Jurassic
Lower Jurassic
Upper Triassic
Lower Triassic
Carboniferous
5 km

1189

Figure 16: Examples of the main trap types observed in the basins offshore southern and eastern Ireland. A) Inversion structure (Seven Heads gas field), B) Tilted fault blocks (Helvick oil discovery) and C) Salt pillows.

Titled fault blocks are also present throughout these basins, having formed during Triassic to Cretaceous rifting. Some of the normal faults bounding these structures were later reactivated with minor reverse motion (*i.e.* remaining net normal faults) during the Cenozoic (Rodríguez-Salgado *et al.*, 2022b). In the North Celtic Sea Basin, the effectiveness of this trap type has been proven by the undeveloped Helvick oil discovery which consists of oil accumulations in Middle to Upper Jurassic reservoirs (Fig. 16B; Caston, 1995). Salt-related structural traps are less common in the basins offshore southern and eastern Ireland as only the Upper Triassic section contains salt, although some salt pillows and anticlines are observed (Merlin Energy Resources Consortium, 2020; Fig. 16C). A faulted, salt-cored structure on the Irish-UK maritime border hosts the undeveloped Dragon gas accumulation in Upper Jurassic sandstones, suggesting these structures could represent viable traps for subsurface fluid storage.

Two basins in the adjacent UK sector are set to host subsurface storage projects and represent good analogues to Irish basins discussed above. The first of these is the East Irish Sea Basin where several older hydrocarbon fields are being proposed for CO_2 storage *(e.g.* Lewis *et al.*, 2009). These hydrocarbon accumulations are found in a similar geological setting to the Triassic storage play in the Slyne and Erris basins, with a Lower Triassic sandstone reservoir sealed by Upper Triassic halite interbedded with mudstones, although the Permian section composed of clastic and carbonate rocks compared to the salt-prone section offshore Ireland. This basin has undergone a more complex post-rift evolution involving trap modification and local depressurisation due to glacial loading and unloading (Williams *et al.*, 2018). As discussed above, halite in the Upper Triassic was crucial in preserving hydrocarbon accumulations during periods of tectonic and glacial modification, indicating its importance for long-term subsurface storage in similar basins like those offshore northwestern Ireland (Seedhouse and Racey, 1997).

The second relevant basin is the Larne Basin (also referred to as the Antrim Basin and Ulster Basin) which underlies both the eastern coast of Northern Ireland and the North Channel (Fyfe *et al.*, 2020). This basin contains a Triassic reservoir-seal pair consisting of a Lower Triassic sandstone overlain by Upper Triassic mudstone and salt, equivalent to that in the Slyne and Erris basins (Illing and Griffith, 1986). These are underlain locally by a Permian salt layer (the Belfast Harbour Evaporite Formation) which is similar to that found in the Slyne and Erris basins. The Islandmagee Gas Storage Project aims to create up to seven artificial salt caverns beneath Larne Lough in this Permian salt to store either natural gas or hydrogen (Islandmagee Energy, 2023). Further site characterisation will be needed before the project can proceed, both to understand the salt layers, which include Cenozoic igneous intrusions as possible leakage points (Andeskie and Benison, 2021), and to address the societal and environmental concerns of the local communities.

8.5 Comparison with other methodologies applied to the Irish Atlantic margin

Two previous studies have assessed the potential of basins and structures on the Irish Atlantic margin for CO_2 storage: Lewis *et al.* (2009) and English and English (2022). Lewis *et al.* (2009) carried out an all-island assessment of the Upper Paleozoic and Mesozoic basins located onshore and offshore Ireland. A large portion of the data available for our present study was confidential at the time and so those authors classified the capacity for the Slyne and Erris basins as unknown and did not provide a storage volume estimate (Lewis *et al.*, 2009). No reference was made to the Donegal Basin in that study. Lewis *et al.* (2009) used a modified FIP equation (*e.g.* Calhoun, 1976) for calculating saline aquifer capacity for other basins in the Irish and Celtic seas:

$$CO_2\ storage\ capacity = total\ pore\ volume\ \times density\ of\ CO_2\ \times 0.4$$

Lewis *et al.* (2009) calculated the total pore volume with an average porosity and net-to-gross values throughout the basin while using the whole area of the basin and an average reservoir thickness to calculate gross rock volume. They used a value of 0.4 to account for the fluid dynamics of CO_2 resulting in relatively low fluid saturation. While this method allows rapid estimation of the total potential capacity of a basin, it does not identify structural traps or account for lateral (*i.e.* net-to-gross) and vertical (*i.e.* porosity) changes in geology within the basin.

Both Lewis *et al.* (2009) and English and English (2022) applied the equation for depleted gas reservoirs presented by Bachu and Shaw (2003) for estimating CO_2 storage capacity in Ireland's gas fields:

$$CO_2\ storage\ capacity = \left({V_g(sc)}/{FVF}\right) \times density\ of\ CO_2$$

Where $V_g(sc)$ is the ultimate volume of recoverable gas at standard conditions and FVF is the gas formation volume factor, representing the ratio of volume at reservoir and standard conditions. Using this equation, English and English (2022) calculated a CO_2 capacity of 44 million tonnes for the Lower Triassic reservoir in the Corrib gas field, including a discount factor of 0.65 to account for water invasion during initial gas production. This is similar to the P50 value calculated in this study for the Corrib Triassic storage play using the initial gas-water contact as the closing contour (54 million tonnes, Table 2). The similarity in the values for CO_2 storage capacity also indicates that these methods represent theoretical storage volumes rather than effective storage volumes as previously discussed.

Recent publications have also investigated the potential of Ireland's sedimentary basins to host subsurface hydrogen storage sites (Dinh, *et al.*, 2021; Xiao *et al.*, 2022; English and English, 2023). These authors identified the geology of the basins offshore north-western Ireland as being suitable for further investigation. English and English (2023) also applied a modified version of Bachu and Shaw's (2003) equation for depleted gas fields to assess the volume of working gas capacity of the Corrib gas field. They calculated a similar value (37.7 TWh) to the P50 calculated for the Corrib Triassic storage play (Table 2) using the initial gas-water contact as the closing contour in this study (32 TWh). The reasonable representation of the volumes for CO_2 and H_2 capacity at Corrib using the methodology of this study compared with those of Bachu and Shaw (2003) indicates that other structures in the subsurface in the Slyne, Erris and Donegal basins are also likely to be reasonably represented using this methodology.

The methods used in this study provide better estimates of subsurface storage volumes in underexplored regions like the Irish Atlantic margin. The methods of Lewis *et al.* (2009) are most applicable to a basin-by-basin comparison for estimating basin-wide fluid storage capacity but do not account for the lateral and vertical changes in intra-basinal geology and lack the spill-point analysis component to identify structural closures within a particular basin. Bachu and Shaw's (2003) method for estimating volumes in depleted gas fields used by both Lewis *et al.* (2009) and English and English (2022) relies on existing developed gas accumulations, making it a very powerful tool in mature oil and gas provinces such as the North Sea and East Irish Sea along with specific fields like the Corrib gas field, but less so in underexplored areas like the sedimentary basins offshore Ireland.

8.5. Linking subsurface storage with other infrastructure on the Irish Atlantic margin

This study has primarily considered the geological factors influencing the suitability of different structures to act as subsurface storage sites. Other factors including the distance from potential offshore renewable energy generation sites or high CO_2 emitters are important when considering the development of offshore storage facilities. The largest hurdle to CO_2 storage in Ireland at time of writing is legislation; Article 4 of the European Communities (Geological Storage of Carbon Dioxide) Regulations (2011) states 'the storage of CO_2 in a storage site in part or in the whole of [the territory, exclusive economic zone and the continental shelf of the Republic of Ireland] is not permitted'. Therefore, changes to this legislation will need to take place before any CO_2 storage projects are developed in Ireland. Nevertheless, given the increasing drive to reduce greenhouse gas concentrations in the atmosphere, non-geological factors which will be important to offshore gas storage projects are discussed below.

Two of Ireland's largest point-source CO_2 emitters (Moneypoint power station and Aughinish Alumina) are located on the western coast of the country (Table 5; Fig. 17; European Commission, 2022). Local storage plays in the Southern Slyne sub-basin (*e.g.* the Inishmore structure) may therefore make suitable storage locations for CO_2 generated from these large point-source emitters. Indigenous sources of CO_2 could be supplemented by international sources with the adoption of international CO_2 shipping (Al Baroudi et al, 2021). This would allow Ireland to receive shipments of CO_2 and store these in structural traps in the basins on the Irish Atlantic margin. This may be further aided by changes to the EU Emission Trading System to incorporate negative emissions from CCS projects to provide more incentive for the development of carbon storage facilities (*e.g.* Rickels *et al.*, 2021).

Table 5: 25 largest CO_2 emitters in Ireland in 2021 (European Commission, 2022). Note IDs 1, 18 and 19 are not point source emitters.

ID	Emitting entity	Type of activity	Verified emissions 2021 (tonnes of CO_2)
1	Ryanair DAC	Aircraft operator	4941568
2	ESB Moneypoint Generating Station	Coal-fired power station	3228756
3	Aughinish Alumina	Alumina refinery	1185891
4	Irish Cement Limited (Platin Works)	Cement manufacturer	1065759
5	Great Island Generating Station	CCGT power station	993092

6	Scotchtown Cement Works	Cement manufacturer	849233
7	Aghada CCGT	CCGT power station	807993
8	Huntstown Power Station	CCGT power station	775793
9	Tynagh 400MW CCPP	CCGT power station	773138
10	Irish Cement Limited (Limerick Works)	Cement manufacturer	766035
11	Dublin Bay Power Plant	CCGT power station	679932
12	ESB Poolbeg Generating Station (CCGT)	CCGT power station	659638
13	Tarbert Generating Station	Oil-fired power station	485972
14	Breedon Cement Ireland Limited	Cement manufacturer	453868
15	Edenderry Power Plant	Peat and biomass-fired power station	334945
16	Irving Oil Whitegate Refinery Limited	Oil refinery	294148
17	CCGT HPC2 (Huntstown Power Station Phase II)	CCGT power station	190841
18	Aer Lingus Limited AOHA	Aircraft operator	161319
19	ASL Airlines (Ireland) Limited	Aircraft operator	160526
20	Premier Periclase Limited	Magnesia-product manufacturer	104703
21	Glanbia Ireland DAC Ballyragget	Dairy products manufacturer	85471
22	Clogrennane Lime Limited (Toonagh Lime Works)	Lime manufacturer	82164
23	Bord na Mona Derrinlough Briquette Factory	Briquette manufacturer	75845
24	Bailieboro Foods Limited	Dairy products manufacturer	75139
25	Whitegate Power Station	CCGT power station	64239

The development of major offshore wind projects along Ireland's western and north-western coastlines (Fig. 17) may provide synergistic opportunities to explore the subsurface energy storage potential of the Slyne, Erris and Donegal basins. This could involve power-to-gas schemes, using excess electricity to generate either H_2 fuel or to inject compressed air into storage sites in these basins, providing deployable energy to meet national demand. These synergies have recently been explored in the North Sea and East Irish Sea basins in the UK and at the Kinsale Head gas field offshore southern Ireland (*e.g.* O'Kelly-Lynch *et al.*, 2020; Peecock *et al.*, 2023). Linked developments offshore northwestern Ireland could include the proposed offshore wind developments to the west of the Shannon Estuary and in Donegal Bay linked with structures in the Slyne and Erris basins (Fig. 17; 4C Offshore, 2023). Offshore wind developments to the north of Ireland and the west of Scotland in the Malin Sea (Fig. 17; 4C Offshore, 2023) could be partnered with storage sites in the Donegal Basin (*e.g.* Inishbeg), through cross-border collaboration, or linked with structural closures identified in the Rathlin Trough and North Channel basins (*e.g.* Quinn *et al.*, 2010; Fyfe *et al.*, 2020).

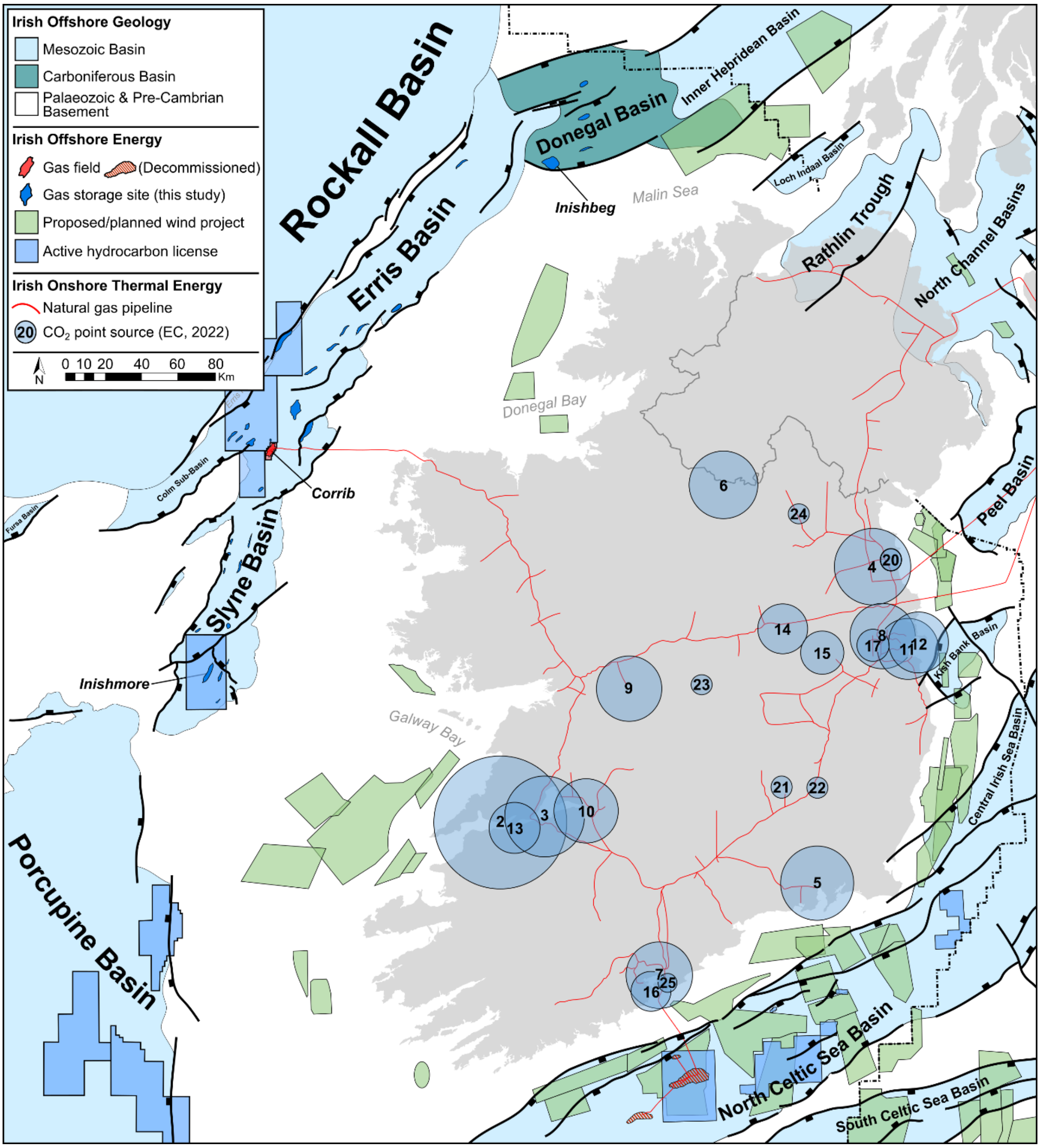

***Figure 17:** Overview map of energy infrastructure on- and offshore Ireland. Size of CO_2 point source emitters (note IDs 1, 18 and 19 are not point source emitters and are excluded here) proportional to scale of emissions (see Table 5). CO_2 emission data and locations from European Commission (2022). Proposed offshore wind development polygons are adapted from 4C Offshore (2023). Celtic and Irish Sea basins adapted from Rodriguez-Salgado et al. (2022b). Porcupine Basin outline adapted from Saqab et al. (2020). Northern Irish and Scottish basins adapted from Fyfe et al. (2020).*

The presence of existing subsea infrastructure will accelerate the development of offshore energy projects through reengineering and reuse. The decommissioned Kinsale Head gas field in the North Celtic Sea Basin (Fig. 17) is being actively investigated for its potential to store H_2 using existing infrastructure (ESB, 2021). In the basins offshore north-western Ireland investigated in this study, the Corrib gas field represents one of the most attractive sites for further development as existing infrastructure can be repurposed for the storage and withdrawal of different fluids when natural gas production finishes (*e.g.* DNV, 2021). This would significantly reduce capital expenditure when compared to a greenfield offshore storage site. Sites that are located near the Corrib gas field in the Northern Slyne sub-basin and the Southern Erris sub-basin could also benefit from their proximity to this existing infrastructure with development incentives like near-field exploration strategies employed in hydrocarbon exploration (*e.g.* Marchant *et al.*, 2001; Hulsey *et al.*, 2019). Therefore, it is likely that should gas storage sites be developed in the sedimentary basins offshore north-western Ireland, those near existing subsea infrastructure will be the first to be investigated.

9. Conclusions

A simplified workflow for charactering reservoirs and estimating subsurface storage volumes is scalable across areas with different levels of data coverage has been adapted from existing hydrocarbon exploration methods. It can incorporate a wide range of geological and engineering data to identify storage sites and estimate volumes. Estimates for storage volumes were calculated using a Fluid In Place equation for two fluid types (CO_2 and H_2). This is a suitable workflow to quickly identify a portfolio of prospective storage sites throughout a basin or group of basins that can scale from data-poor to data-dense areas. While not done in this study, a quantitative multi-criterion ranking scheme such as Quantitative SWOT or TOPSIS analyses would then identify the most suitable sites for further investigation. Finally, should the focus of a regional study narrow to just storage of CO_2, then additional consideration will need to be given to both the storage efficiency factor and both local and regional aquifer volume and how pressure changes can lead to overpressure and seal failure.

This workflow was applied to the Slyne, Erris and Donegal basins offshore northwestern Ireland with the following results:

- Three storage plays have been characterised. They consist of Carboniferous, Lower Triassic and Upper Jurassic sandstone reservoirs sealed by interbedded Carboniferous mudstones and Permian salt, Upper Triassic salt and mudstone, and interbedded Upper Jurassic mudstones respectively. Of these, the Lower Triassic sandstones have the highest porosity and permeabilities, greatest net-to-gross ratios, and the most effective seal.
- All three of these storage plays could effectively host CO_2 in structural traps for geological periods of time. The Lower Triassic storage play is the most suitable for H_2 storage where it is overlain by Upper Triassic salt. The Carboniferous storage play is a second viable candidate where it is overlain by Permian salt although it typically has poorer reservoir properties.
- Salt seals are considered to offer the lowest risk potential for the long-term storage of fluids in the subsurface (*i.e.* CO_2). This is demonstrated both offshore northwestern Ireland and in the East Irish Sea Basin where a salt seal has preserved fluid accumulations in structural traps despite subsequent tectonic and glacial modification. These salt layers also offer potential sites for artificial salt cavern formation. While the extent of these salt layers has been recently mapped using seismic reflection data

coupled with the few available boreholes, more work will be needed to understand the distribution and composition of these layers and any interbedded impurities.
- Evidence of hydrocarbon leakage in the form of breached accumulations and seabed pockmarks highlight the importance of caprock, fault seal, and fault stability analyses during the characterisation of these storage sites.

Alongside the three basins and three storage plays investigated in this study, there is significant storage resource potential on and around the island of Ireland that warrants further investigation. As Ireland looks to progress its renewable energy ambitions, its sedimentary basins offer significant potential for both collaborative energy and CO_2 storage. The presence of existing subsea and onshore infrastructure at the Corrib gas field makes it an ideal candidate for further feasibility study and provides an incentive for infrastructure-led exploration for additional storage volume offshore northwest Ireland.

Acknowledgements:

This research was funded in part by a research grant from Science Foundation Ireland (SFI) under Grant Number 13/RC/2092 and was co-funded under the European Regional Development Fund, and by the Petroleum Infrastructure Programme (PIP) and its member companies. Muhammad Mudasar Saqab and John Walsh are thanked for supervision during early stages of this project. The authors would like to thank Ciaran Nolan and Martin Grecula for their constructive reviews together with the editorial guidance of Graham Goffey. The authors would like to thank the Petroleum Affairs Division (PAD) of the Department of Environment, Climate and Communications (DECC), Ireland, for providing access to seismic reflection and borehole datasets. Shell Exploration and Production Ireland Ltd. are thanked for providing access to reprocessed volumes of the 1997 Corrib 3D. The authors would also like to thank Schlumberger for providing academic licenses of Petrel to University College Dublin. SINTEF Digital is thanked for providing access to the open-source MRST-co2lab software. The colour maps used for surface elevation maps are developed by Fabio Crameri.

References:

4C Offshore. 2023. Global Offshore Renewable Database. Available at https://map.4coffshore.com/offshorewind/. Accessed 14/04/2023.

Agada, S., Jackson, S., Kolster, C., MacDowell, N., Williams, G., Vosper, H., Williams, J. and Krevor, S. 2017. The impact of energy systems demands on pressure limited CO2 storage in the Bunter Sandstone of the UK Southern North Sea. International Journal of Greenhouse Gas Control, 65, 128–136, https://doi.org/10.1016/j.ijggc.2017.08.014.

Agartan, E., Gaddipati, M., Yip, Y., Savage, B. and Ozgen, C. 2018. CO2 storage in depleted oil and gas fields in the Gulf of Mexico. International Journal of Greenhouse Gas Control, 72, 38–48, https://doi.org/10.1016/j.ijggc.2018.02.022.

Al Baroudi, H., Awoyomi, A., Patchigolla, K., Jonnalagadda, K. and Anthony, E.J. 2021. A review of large-scale CO2 shipping and marine emissions management for carbon capture, utilisation and storage. Applied Energy, 287, 116510, https://doi.org/10.1016/j.apenergy.2021.116510.

Alcalde, J., Heinemann, N., James, A., Bond, C.E., Ghanbari, S., Mackay, E.J., Haszeldine, R.S., Faulkner, D.R., Worden, R.H. and Allen, M.J. 2021. A criteria-driven approach to the CO2 storage site selection of East Mey for the acorn project in the North Sea. Marine and Petroleum Geology, 133, 105309, https://doi.org/10.1016/j.marpetgeo.2021.105309.

Amoco 1978. Well 19/5-1 Geological Completion Report. Amoco Ireland Exploration Company, compiled by Odell, R.T. and Thomas, I.W.

Amoco 1979. Wells 12/13-1 and 12/13-1A Geological Completion Report. Amoco Ireland Exploration Company, compiled by Odell, R.T. and Walker, D.

Andeskie, A.S. and Benison, K.C. 2021. A missing link in the mid-late Permian record of north-eastern Pangea: A sedimentological evaluation of the Permian Belfast Harbour Evaporite Formation of County Antrim, Northern Ireland. Depositional Record, 7, 451–469, https://doi.org/10.1002/dep2.144.

Asquith, G., Krygowski, D., Henderson, S. and Hurley, N. 2004. Gamma Ray Log. In: Basic Well Log Analysis. 31–35., https://doi.org/10.1306/Mth16823C3.

Bachu, S. and Shaw, J. 2003. Evaluation of the CO2 Sequestration Capacity in Alberta's Oil and Gas Reservoirs at Depletion and the Effect of Underlying Aquifers. Journal of Canadian Petroleum Technology, 42, 51–61, https://doi.org/10.2118/03-09-02.

Bachu, S. 2015. Review of CO2 storage efficiency in deep saline aquifers. International Journal of Greenhouse Gas Control, 40, 188–202, https://doi.org/10.1016/j.ijggc.2015.01.007.

Bérest, P., Réveillère, A., Evans, D. and Stöwer, M. 2019. Review and analysis of historical leakages from storage salt caverns wells. *Oil & Gas Science and Technology – Revue d'IFP Energies Nouvelles*, **74**, 27, https://doi.org/10.2516/ogst/2018093.

Biancotto, F., Hardy, R.J.J., Jones, S.M., Brennan, D. and White, N.J. 2007. Estimating denudation from seismic velocities offshore NW Ireland. Society of Exploration

Geophysicists – 77th SEG International Exposition and Annual Meeting, SEG 2007, 407–411.

Bickle, M.J. 2009. Geological carbon storage. Nature Geoscience, 2, 815–818, https://doi.org/10.1038/ngeo687.

Blunt, M., Fayers, F.J. and Orr, F.M. 1993. Carbon dioxide in enhanced oil recovery. Energy Conversion and Management, 34, 1197–1204, https://doi.org/10.1016/0196-8904(93)90069-M.

Bui, M., Adjiman, C.S., Bardow, A., Anthony, E.J., Boston, A., Brown, S., Fennell, P.S, Fuss, S., Galindo, A., Hackett, L.A., Hallett, J.P., Herzog, H.J., Jackson, G., Kemper, J., Krevor, S., Maitland, G.C., Matuszewski, M., Metcalfe, I.S., Petit, C., Puxty, G., Reimer, J., Reiner, D.M., Rubin, E.S., Scott, S.A., Shah, N., Smit, B., Martin Trusler, J.P., Webley, P., Wilcox, J. and Mac Dowell, N. 2018. Carbon capture and storage (CCS): The way forward. Energy and Environmental Science, 11, 1062–1176, https://doi.org/10.1039/c7ee02342a.

Calhoun Jr, J.C. 1976. Fundamentals of reservoir engineering.

Casacão, J., Silva, F., Rocha, J., Almeida, J. and Santos, M. 2023. Aspects of salt diapirism and structural evolution of Mesozoic–Cenozoic basins at the West Iberian margin. AAPG Bulletin, 107, 49–85, https://doi.org/10.1306/08072221100.

Caston, V., 1995, The Helvick oil accumulation, Block 49/9, North Celtic Sea Basin: Geological Society, London, Special Publications, v. 93, no. 1, p. 209-225.

Chapman, T.J., Broks, T.M., Corcoran, D. V., Duncan, L.A. and Dancer, P.N. 1999. The structural evolution of the Erris Trough, offshore northwest Ireland, and implications for hydrocarbon generation. Petroleum Geology of Northwest Europe: Proceedings of the 5th Conference, 455–469.

Chock, R.Y., Miller, W.B., King, S.N.D, Brehme, C.S., Fisher, R.N., Sin, H., Wilcox, P., Terp, J., Tremor, S., Major, M.R., Merrill, K., Spencer, W.D., Sullivan, S. and Shier, D.M. 2022. Quantitative SWOT analysis: A structured and collaborative approach to reintroduction site selection for the endangered Pacific pocket mouse. Journal for Nature Conservation, 70, 126268, https://doi.org/10.1016/j.jnc.2022.126268.

Clark, C.D., Ely, J.C., Hindmarhs, R.C.A., Bradley, S., Ignéczi, A., Fabel, D., Ó Cofaigh, C., Chiverrell, R.C., Scourse, J., Benetti, S., Bradwell, T., Evans, D.J.A., Roberts, D.H., Burke, M., Callard, S.L., Medialdea, A., Saher, M., Small, D., Smedley, R.K., Gasson, E., Gregoire, L., Gandy, N., Hughes, A.L.C., Ballantyne, C., Bateman, M.D., Bigg, G.R., Doole, J., Dove, D., Duller, G.A.T., Jenkins, G.T.H., Livingstone, S.L., McCarron, S., Moreton, S., Pollard, D., Praeg, D., Serjup, H.P., Van Landeghem, K.J.J. and Wilson, P. 2022. Growth and retreat of the last British–Irish Ice Sheet, 31 000 to 15 000 years ago: the BRITICE-CHRONO reconstruction. Boreas, 51, 699–758, https://doi.org/10.1111/bor.12594.

Corcoran, D.V. and Clayton, G. 2001. Interpretation of vitrinite reflectance profiles in sedimentary basins, onshore and offshore Ireland. Geological Society, London, Special Publications, 188, 61–90, https://doi.org/10.1144/GSL.SP.2001.188.01.04.

Corcoran, D.V. and Doré, A.G. 2002. Depressurization of hydrocarbon-bearing reservoirs in exhumed basin settings: evidence from Atlantic margin and borderland basins. Geological Society, London, Special Publications, 196, 457–483, https://doi.org/10.1144/GSL.SP.2002.196.01.25.

Corcoran, D.V. and Mecklenburgh, R. 2005. Exhumation of the Corrib Gas Field, Slyne Basin, offshore Ireland. Petroleum Geoscience, 11, 239–256, https://doi.org/10.1144/1354-079304-637.

Crotogino, F. 2022. Large-Scale Hydrogen Storage, https://doi.org/10.1016/B978-0-12-824510-1.00003-9.

Dancer, P.N., Algar, S.T. and Wilson, I.R. 1999. Structural evolution of the Slyne Trough. Petroleum Geology of Northwest Europe: Proceedings of the 5th Conference on the Petroleum Geology of Northwest Europe, 1, 445–454, https://doi.org/10.1144/0050729.

Dancer, P.N., Kenyon-Roberts, S.M., Downey, J.W., Baillie, J.M., Meadows, N.S. and Maguire, K. 2005. The Corrib gas field, offshore west of Ireland. Geological Society, London, Petroleum Geology Conference series, 6, 1035–1046, https://doi.org/10.1144/0061035.

Dawood, F., Anda, M. and Shafiullah, G.M. 2020. Hydrogen production for energy: An overview. International Journal of Hydrogen Energy, 45, 3847–3869, https://doi.org/10.1016/j.ijhydene.2019.12.059.

Dincer, I. 2012. Green methods for hydrogen production. International Journal of Hydrogen Energy, 37, 1954–1971, https://doi.org/10.1016/j.ijhydene.2011.03.173.

DNV. 2021. Re-Stream - Study on the Reuse of Oil and Gas Infrastructure for Hydrogen and CCS in Europe.

Dobson, M.R. and Whittington, R.J. 1992. Aspects of the geology of the Malin Sea area. *Geological Society, London, Special Publications*, **62**, 291–311, https://doi.org/10.1144/GSL.SP.1992.062.01.23.

Doré, A.G., Lundin, E.R., Jensen, L.N., Birkeland, O., Eliassen, P.E. and Fichler, C. 1999. Principal tectonic events in the evolution of the northwest European Atlantic margin. Petroleum Geology of Northwest Europe: Proceedings of the 5th Conference, 41–61.

Duffy, O.B., Hudec, M.R., Peel, F., Apps, G., Bump, A., Moscardelli, L., Dooley, T.P., Fernandez, N., Bhattacharya, S., Wisian, K. and Shuster, M.W. 2022. The Role of Salt Tectonics in the Energy Transition: An Overview and Future Challenges Running Title: Salt Tectonics and the Energy Transition. Tektonika, 1.

Duncan, W.I., Green, P.F. and Duddy, I.R. 1998. Source rock burial history and seal effectiveness: key facets to understanding hydrocarbon exploration potential in the east and central Irish Sea basins. AAPG Bulletin, 82, 1401–1415.

Dunford, G.M., Dancer, P.N. and Long, K.D. 2001. Hydrocarbon potential of the Kish Bank Basin: Integration within a regional model for the Greater Irish Sea Basin. Geological Society Special Publication, 188, 135–154, https://doi.org/10.1144/GSL.SP.2001.188.01.07.

Edwards B.K. 2003. The economics of hydroelectric power. Edward Edgar Publishing.

Eiken, O., Ringrose, P., Hermanrud, C., Nazarian, B., Torp, T.A. and Høier, L. 2011. Lessons Learned from 14 years of CCS Operations: Sleipner, In Salah and

Snøhvit. Energy Procedia, 4, 5541–5548, https://doi.org/10.1016/j.egypro.2011.02.541.

English, J. M., and English, K. L., 2022, Carbon Capture and Storage Potential in Ireland—Returning Carbon Whence It Came: First Break, v. 40, no. 5, p. 35-43.

Enterprise 1996a. Well IRE 27/5-1 Geological Completion Report. Enterprise Oil plc, compiled by Rawlinson, A., Verlander, J., Scotchman, I. and Henderson, G.

Enterprise 1996b. Well IRE 18/20-1 Geological Completion Report. Enterprise Oil plc, compiled by O'Neill, N., Scotchman, I. and Dancer, N.

Enterprise 2000. Well IRE 18/25-2 Geological Completion Report. Enterprise Oil plc, compiled by Pay, M. and Geerlings, P.

ESB. 2021. ESB and dCarbonX launch Kinsale Head Hydrogen Storage project. Available at: https://esb.ie/media-centre-news/press-releases/article/2021/08/12/esb-and-dcarbonx-launch-kinsale-head-hydrogen-storage-project/ . Accessed: 03/11/2022

European Communities (Geological Storage of Carbon Dioxide) Regulations 2011. 2011. Statutory Instruments Number 575/2011.

European Commission. 2022. The EU emissions trading system (EU ETS). Directorate-General for Climate Action, Publications Office.

Fugro. 1994. Field Report Irish Frontier Shallow Coring Project Blocks 19/13 and 27/24 Irish Sector Atlantic Ocean (Volume II).

Fyfe, L.-J.C., Schofield, N., Holford, S.P., Heafford, A. and Raine, R. 2020. Geology and petroleum prospectivity of the Larne and Portpatrick basins, North Channel, offshore SW Scotland and Northern Ireland. Petroleum Geoscience, https://doi.org/10.1144/petgeo2019-134.

Garcia, X., Monteys, X., Evans, R.L. and Szpak, M. 2014. Constraints on a shallow offshore gas environment determined by a multidisciplinary geophysical approach: The Malin Sea, NW Ireland. Geochemistry, Geophysics, Geosystems, 15, 867–885, https://doi.org/10.1002/2013GC005108.

Godec, M., Kuuskraa, V., Van Leeuwen, T., Melzer, L.S. and Wildgust, N. 2011. CO2 storage in depleted oil fields: The worldwide potential for carbon dioxide enhanced oil recovery. Energy Procedia, 4, 2162–2169, https://doi.org/10.1016/j.egypro.2011.02.102.

Goffey, G., Attree, M., Curtis, P., Goodfellow, F., Lynch, J., Mackertich, D., Orife, T. and Tyrrell, W. 2018. New exploration discoveries in a mature basin: offshore Denmark. Geological Society, London, Petroleum Geology Conference Series, 8, 287–306, https://doi.org/10.1144/PGC8.1.

Hashemi, L., Blunt, M. and Hajibeygi, H. 2021. Pore-scale modelling and sensitivity analyses of hydrogen-brine multiphase flow in geological porous media. Scientific Reports, 11, 1–13, https://doi.org/10.1038/s41598-021-87490-7.

Heinemann, N., Booth, M.G., Haszeldine, R.S., Wilkinson, M., Scafidi, J. and Edlmann, K. 2018. Hydrogen storage in porous geological formations – onshore play opportunities in the midland valley (Scotland, UK). International Journal of

Hydrogen Energy, 43, 20861–20874, https://doi.org/10.1016/j.ijhydene.2018.09.149.

Holdsworth, R.E., McCaffrey, K.J.W., Dempsey, E., Roberts, N.M.W., Hardman, K., Morton, A., Feely, M., Hunt, J., Conway, A. and Robertson, A. 2019. Natural fracture propping and earthquake-induced oil migration in fractured basement reservoirs. Geology, 47, 700–704, https://doi.org/10.1130/g46280.1.

Holford, S. P., Turner, J. P., and Green, P. F. 2005. Reconstructing the Mesozoic–Cenozoic exhumation history of the Irish Sea basin system using apatite fission track analysis and vitrinite reflectance data. In Geological Society, London, Petroleum Geology Conference series (Vol. 6, No. 1, pp. 1095-1107). Geological Society of London.

Holloway, S., Vincent, C.J., Bentham, M.S. and Kirk, K.L. 2006. Top-down and bottom-up estimates of CO2 storage capacity in the United Kingdom sector of the southern North Sea basin. Environmental Geosciences, 13, 71–84, https://doi.org/10.1306/eg.11080505015.

Howard, A., Beswetherick, S. and Miglio, G. 2009. Prospectivity on the Erris Ridge (Licence 7/97)—High Risk/High Reward Frontier Exploration on the Irish Atlantic Margin. In: Offshore Europe, https://doi.org/10.2118/125073-MS.

Hudec, M.R. and Jackson, M.P.A. 2007. Terra infirma: Understanding salt tectonics. Earth-Science Reviews, 82, 1–28, https://doi.org/10.1016/j.earscirev.2007.01.001.

Hulsey, J., Bernaez, A., Strickland, B. and Cook, A. 2019. Workflows for near-field exploration. Interpretation, 7, T595–T606, https://doi.org/10.1190/INT-2018-0200.1.

IEA. 2018. Whatever happened to enhanced oil recovery?, International Energy Agency, Paris. Available at: https://www.iea.org/commentaries/whatever-happened-to-enhanced-oil-recovery. Accessed 15/06/2023

IEA. 2022. Hydrogen. International Energy Agency, Paris. Available at: https://www.iea.org/reports/hydrogen. Accessed 15/06/2023

Iglauer, S. 2022. Optimum geological storage depths for structural H2 geo-storage. Journal of Petroleum Science and Engineering, 212, 109498, https://doi.org/10.1016/j.petrol.2021.109498.

Illing, L. V and Griffith, A.E. 1986. Gas Prospects in the ‘Midland Valley’ of Northern Ireland. Geological Society, London, Special Publications, 23, 73–84, https://doi.org/10.1144/GSL.SP.1986.023.01.05.

IPCC, 2022: Climate Change 2022: Mitigation of Climate Change. Contribution of Working Group III to the Sixth Assessment Report of the Intergovernmental Panel on Climate Change. P.R. Shukla, J. Skea, R. Slade, A. Al Khourdajie, R. van Diemen, D. McCollum, M. Pathak, S. Some, P. Vyas, R. Fradera, M. Belkacemi, A. Hasija, G. Lisboa, S. Luz, J. Malley, (eds.). Cambridge University Press, Cambridge, UK and New York, NY, USA. https://doi.org/10.1017/9781009157926

Islandmagee Energy. 2023. Islandmagee Energy – Gas storage facility. Available at https://www.islandmageeenergy.com/. Accessed 12/12/2023.

Jackson, M.P.A. and Hudec, M.R. 2017a. Salt Pillows and Salt Anticlines. *In*: *Salt Tectonics*. 62–75., https://doi.org/10.1017/9781139003988.007.

Jackson, M.P.A. and Hudec, M.R. 2017b. Salt Stocks and Salt Walls. *In*: *Salt Tectonics*. 76–118., https://doi.org/10.1017/9781139003988.008.

Klempa, M., Ryba, J. and Bujok, P. 2019. The storage capacity of underground gas storages in the Czech Republic. *GeoScience Engineering*, **65**, 18–25, https://doi.org/10.35180/gse-2019-0014.

Krevor, S.C.M., Pini, R., Zuo, L. and Benson, S.M. 2012. Relative permeability and trapping of CO2 and water in sandstone rocks at reservoir conditions. Water Resources Research, 48, 1–16, https://doi.org/10.1029/2011WR010859.

Lange, M., O'Hagan, A.M., Devoy, R.R.N., Le Tissier, M. and Cummins, V. 2018. Governance barriers to sustainable energy transitions – Assessing Ireland's capacity towards marine energy futures. Energy Policy, 113, 623–632, https://doi.org/10.1016/j.enpol.2017.11.020.

Lau, H.C., Ramakrishna, S., Zhang, K. and Radhamani, A.V. 2021. The role of carbon capture and storage in the energy transition. Energy and Fuels, 35, 7364–7386, https://doi.org/10.1021/acs.energyfuels.1c00032.

Lech, M.E., Jorgensen, D.C., Southby, C., Wang, L., Nguyen, V., Borissova, I. and Lescinsky, D. 2016. Palaeogeographic mapping to understand the hydrocarbon and CO2 storage potential of the post-rift Warnbro Group, offshore Vlaming Sub-basin, southern Perth Basin, Australia. Marine and Petroleum Geology, 77, 1206–1226, https://doi.org/10.1016/j.marpetgeo.2016.03.014.

Lewis, D., Bentham, M., Cleary, T., Vernon, R., O'Neill, N., Kirk, K., Chadwick, A., Hilditch, D., Michael, K., Allinson, G., Neal, P. and Ho, M. 2009. Assessment of the potential for geological storage of carbon dioxide in Ireland and Northern Ireland. Energy Procedia, 1, 2655–2662, https://doi.org/10.1016/j.egypro.2009.02.033.

Linstrom, P.J. and Mallard, W.G. 2022. NIST Chemistry WebBook, NIST Standard Reference Database Number 69, National Institute of Standards and Technology. https://doi.org/10.18434/T4D303

Lloyd, C., Huuse, M., Barrett, B.J. and Newton, A.M.W. 2021. Regional Exploration and Characterisation of CO2 Storage Prospects in the Utsira-Skade Aquifer, North Viking Graben, North Sea. Earth Science, Systems and Society, 1, 1–29, https://doi.org/10.3389/esss.2021.10041.

Lothe, A.E., Bergmo, P.E.S. and Grimstad, A.-A. 2019. Storage Resources for Future European CCS Deployment; A Roadmap for A Horda CO2 Storage Hub, Offshore Norway. 10th Trondheim Conference on CO2 Capture, Transport and Storage, 10, 39–48.

Lundin 2006. Well 13/12-1 Inishbeg Prospect End of Well Report. Lundin Britain Ltd., compiled by Craig, D. and Welding, P.

Maddox, S.J., Blow, R. and Hardman, M. 1995. Hydrocarbon prospectivity of the Central Irish Sea Basin with reference to Block 42/12, offshore Ireland. Geological Society Special Publication, 93, 59–77, https://doi.org/10.1144/GSL.SP.1995.093.01.08.

Marchant, T., Wilson, H. and Bamford, D. 2001. Near-Field Exploration: From Failure to Success. In: SPE Annual Technical Conference and Exhibition, https://doi.org/10.2118/71428-MS.

McVay, D.A. and Spivey, J.P. 2001. Optimizing Gas-Storage Reservoir Performance. *SPE Reservoir Evaluation & Engineering*, **4**, 173–178, https://doi.org/10.2118/71867-PA.

Merlin Energy Resources Consortium: The Standard Stratigraphic Nomenclature of Offshore Ireland: An Integrated Lithostratigraphic, Biostratigraphic and Sequence Stratigraphic Framework. Project Atlas. Petroleum Affairs Division, Department of the Environment, Climate and Communications, Special Publication 1/21. 2020.

Metz, B., Davidson, O., De Coninck, H.C., Loos, M. and Meyer, L. 2005. IPCC special report on carbon dioxide capture and storage. Cambridge: Cambridge University Press.

Miocic, J., Heinemann, N., Edlmann, K., Scafidi, J., Molaei, F. and Alcalde, J. 2023. Underground hydrogen storage: a review. Geological Society, London, Special Publications, 528, https://doi.org/10.1144/sp528-2022-88.

Møll Nilsen, H., Lie, K.-A., Møyner, O. and Andersen, O. 2015. Spill-point analysis and structural trapping capacity in saline aquifers using MRST-co2lab. Computers & Geosciences, 75, 33–43, https://doi.org/10.1016/j.cageo.2014.11.002.

Murdoch, L. M., Musgrove, F. W., and Perry, J. S. 1995. Tertiary uplift and inversion history in the North Celtic Sea Basin and its influence on source rock maturity. Geological Society, London, Special Publications, 93(1), 297-319.

Naylor, D. 1983. Petroleum exploration in the Republic of Ireland: A review. Energy exploration & exploitation, 3, 5–26.

Naylor, D. and Shannon, P.M. 1999. The Irish Sea region: Why the general lack of exploration success? Journal of Petroleum Geology, 22, 363–370, https://doi.org/10.1111/j.1747-5457.1999.tb00992.x.

Newborough, M. and Cooley, G. 2020. Developments in the global hydrogen market: The spectrum of hydrogen colours. Fuel Cells Bulletin, 2020, 16–22, https://doi.org/10.1016/S1464-2859(20)30546-0.

O'Kelly-Lynch, P., Gallagher, P., Borthwick, A., McKeogh, E. and Leahy, P. 2020. Offshore conversion of wind power to gaseous fuels: Feasibility study in a depleted gas field. Proceedings of the Institution of Mechanical Engineers, Part A: Journal of Power and Energy, 234, 226–236, https://doi.org/10.1177/0957650919851001.

Oldenburg, C.M. and Doughty, C. 2011. Injection, Flow, and Mixing of CO2 in Porous Media with Residual Gas. Transport in Porous Media, 90, 201–218, https://doi.org/10.1007/s11242-010-9645-1.

Osmond, J.L., Mulrooney, M.J., Holden, N., Skurtveit, E., Faleide, J.I. and Braathen, A. 2022. Structural traps and seals for expanding CO2 storage in the northern Horda platform, North Sea. AAPG Bulletin, 106, 1711–1752, https://doi.org/10.1306/03222221110.

O'Sullivan, C. and Childs, C. 2021. Kinematic interaction between stratigraphically discrete salt layers; the structural evolution of the Corrib gas field, offshore NW

Ireland. Marine and Petroleum Geology, 133, 105274, https://doi.org/10.1016/j.marpetgeo.2021.105274.

O'Sullivan, C.M., Childs, C.J., Saqab, M.M., Walsh, J.J. and Shannon, P.M. 2021. The influence of multiple salt layers on rift-basin development; The Slyne and Erris basins, offshore NW Ireland. Basin Research, 1–31, https://doi.org/10.1111/bre.12546.

O'Sullivan, C.M., Childs, C.J., Saqab, M.M., Walsh, J.J. and Shannon, P.M. 2022. Tectonostratigraphic evolution of the Slyne Basin. Solid Earth, 13, 1649–1671, https://doi.org/10.5194/se-13-1649-2022.

Ozarslan, A. 2012. Large-scale hydrogen energy storage in salt caverns. International Journal of Hydrogen Energy, 37, 14265–14277, https://doi.org/10.1016/j.ijhydene.2012.07.111.

Peecock, A., Edlmann, K., Mouli-Castillo, J., Martinez-Felipe, A. and McKenna, R. 2023. Mapping hydrogen storage capacities of UK offshore hydrocarbon fields and exploring potential synergies with offshore wind. Geological Society, London, Special Publications, 528, https://doi.org/10.1144/SP528-2022-40.

Petroleum Affairs Division. 2005. Petroleum Systems Analysis of the Slyne, Erris and Donegal Basins Offshore Ireland - Digital Atlas.

Philcox, M.E., Baily, H., Clayton, G. and Sevastopulo, G.D. 1992. Evolution of the Carboniferous Lough Allen Basin, Northwest Ireland. Geological Society Special Publication, 62, 203–215, https://doi.org/10.1144/GSL.SP.1992.062.01.18.

Pogge von Strandmann, P.A.E., Burton, K.W., Snæbjörnsdóttir, S.O., Sigfússon, B., Aradóttir, E.S., Gunnarsson, I., Alfredsson, H.A., Mesfin, K.G., Oelkers, E.H. and Gislason, S.R. 2019. Rapid CO_2 mineralisation into calcite at the CarbFix storage site quantified using calcium isotopes. Nature Communications, 10, 1983, https://doi.org/10.1038/s41467-019-10003-8.

PSE Kinsale Energy. 2020. Gas Storage. PSE Kinsale Energy, 22 August 2022. https://www.kinsale-energy.ie/gas-storage. Accessed 19 September 2022.

Quinn, M.F., Smith, K. and Bulat, J. 2010. A geological interpretation of the nearshore area between Belfast Lough and Cushendun, Northern Ireland, utilising a newly acquired 2D seismic dataset to explore for salt layers for possible gas storage within man-made caverns. British Geological Survey Commissioned Report, CR/10/069.

Ramos, A., García-Senz, J., Pedrera, A., Ayala, C., Rubio, F., Peropadre, C. and Mediato, J.F. 2022. Salt control on the kinematic evolution of the Southern Basque-Cantabrian Basin and its underground storage systems (Northern Spain). Tectonophysics, https://doi.org/10.1016/j.tecto.2021.229178.

Rezaei, A., Hassanpouryouzband, A., Molnar, I., Derikvand, Z., Haszeldine, R.S. and Edlmann, K. 2022. Relative Permeability of Hydrogen and Aqueous Brines in Sandstones and Carbonates at Reservoir Conditions. Geophysical Research Letters, 49, https://doi.org/10.1029/2022gl099433.

Rickels, W., Proelß, A., Geden, O., Burhenne, J. and Fridahl, M. 2021. Integrating Carbon Dioxide Removal Into European Emissions Trading. Frontiers in Climate, 3, 1–10, https://doi.org/10.3389/fclim.2021.690023.

Ringrose, P.S. 2018. The CCS hub in Norway: Some insights from 22 years of saline aquifer storage. Energy Procedia, 146, 166–172, https://doi.org/10.1016/j.egypro.2018.07.021.

Ringrose, P. 2020. How to store CO2 underground: Insights from early-mover CCS projects. Springer Briefs in Earth Science **129**. Springer Cham. https://doi.org/10.1007/978-3-030-33113-9

Robertson, B. and Mousavian, M. 2022. The Carbon Capture Crux: Lessons learned. Institute for Energy Economics and Financial Analysis (IEEFA).

Rodríguez-Salgado, P., Childs, C., Shannon, P.M. and Walsh, J.J. 2020. Structural evolution and the partitioning of deformation during basin growth and inversion: A case study from the Mizen Basin Celtic Sea, offshore Ireland. Basin Research, 1–24, https://doi.org/10.1111/bre.12402.

Rodriguez-Salgado, P., Walsh, J. J., Childs, C., and Manzocchi, T. 2022a. Unlocking the CO2 storage potential of the Celtic Sea Basins from hydrocarbon exploration legacy data, in Proceedings 83rd EAGE Conference & Exhibition 2022, Madrid, Spain.

Rodríguez-Salgado, P., Childs, C., Shannon, P.M. and Walsh, J.J. 2022b. Influence of basement fabrics on fault reactivation during rifting and inversion: a case study from the Celtic Sea basins, offshore Ireland. Journal of the Geological Society, 180, 315–338, https://doi.org/10.1144/jgs2022-024.

Roux, J.P., Fitch-Roy, O., Devine-Wright, P. and Ellis, G. 2022. “We could have been leaders”: The rise and fall of offshore wind energy on the political agenda in Ireland. Energy Research and Social Science, 92, 102762, https://doi.org/10.1016/j.erss.2022.102762.

Rowell, P., 1995, Tectono-stratigraphy of the North Celtic Sea Basin: Geological Society, London, Special Publications, v. 93, no. 1, p. 101-137.

Saqab, M.M., Childs, C., Walsh, J. and Delogkos, E. 2020. Multiphase deformation history of the Porcupine Basin, offshore west Ireland. Basin Research, 1–22, https://doi.org/10.1111/bre.12535.

Sclater, J.G. and Christie, P.A.F. 1980. Continental stretching: An explanation of the Post-Mid-Cretaceous subsidence of the central North Sea Basin. Journal of Geophysical Research: Solid Earth, 85, 3711–3739, https://doi.org/10.1029/JB085iB07p03711.

Scotchman, I.C. and Thomas, J.R.W. 1995. Maturity and hydrocarbon generation in the Slyne Trough, northwest Ireland. The Petroleum Geology of Ireland’s Offshore Basins, 93, 385–412, https://doi.org/10.1144/GSL.SP.1995.093.01.30.

Scotchman, I.C., Doré, A.G. and Spencer, A.M. 2018. Petroleum systems and results of exploration on the Atlantic margins of the UK, Faroes & Ireland: what have we learnt? Geological Society, London, Petroleum Geology Conference series, 8, 187–197, https://doi.org/10.1144/PGC8.14.

SEAI, 2022. Energy in Ireland 2022 Report. Sustainable Energy Authority of Ireland.

Seedhouse, J.K. and Racey, A. 1997. Sealing capacity of the Mercia Mudstone Group in the East Irish Sea Basin: Implications for petroleum exploration. Journal of Petroleum Geology, 20, 261–286, https://doi.org/10.1111/j.1747-5457.1997.tb00636.x.

Serica Energy, 2009. Well 27/4-1, 1z Bandon exploration well and sidetrack geological end of well report. Serica Energy plc.

Shannon, P. 1991. The development of Irish offshore sedimentary basins: Journal of the Geological Society, v. 148, no. 1, p. 181-189.

Shannon, P.M. and Naylor, D. 1998. An assessment of Irish offshore basins and petroleum plays. Journal of Petroleum Geology, 21, 125–152, https://doi.org/10.1306/BF9AB7A1-0EB6-11D7-8643000102C1865D.

Shannon, P.M. 2018. Old challenges, new developments and new plays in Irish offshore exploration. Geological Society, London, Petroleum Geology Conference series, 8, 171–185, https://doi.org/10.1144/PGC8.12.

Shell 2011. Exploration Well IRE 18/20-G Wellbores 18/20-sb01 and 18/20-7 Final Well Report Volume 2: Subsurface Section. Shell Exploration and Production Ireland Ltd., compiled by van Koolwijk, M.

Span, R. and Wagner, W. 1996. A new equation of state for carbon dioxide covering the fluid region from the triple-point temperature to 1100 K at pressures up to 800 MPa. Journal of Physical and Chemical Reference Data, 25, 1509–1596, https://doi.org/10.1063/1.555991.

Spencer, A.M. and MacTiernan, B. 2001. Petroleum systems offshore western Ireland in an Atlantic margin context. Geological Society, London, Special Publications, 188, 9–29, https://doi.org/10.1144/GSL.SP.2001.188.01.02.

Statoil 2004. Well 19/11-1 & 1A Final Well Report. Statoil Exploration (Ireland) Ltd., compiled by Hofsøy, R., Skagen, J., Mortensen, H. and Conroy, J.

StatoilHydro 2009. Well 19/8-1 Cashel Prospect End of Well Report. Statoil Exploration (Ireland) Ltd., compiled by MacTiernan, B., Kleppa, S., Hunnes, O., Sigve-Selnes, K. and Igbineweka, O.J.

Takahashi, T., Ohsumi, T., Nakayama, K., Koide, K. and Miida, H. 2009. Estimation of CO_2 Aquifer Storage Potential in Japan. Energy Procedia, 1, 2631–2638, https://doi.org/10.1016/j.egypro.2009.02.030.

Tate, M.P. and Dobson, M.R. 1989. Pre-Mesozoic geology of the western and north-western Irish continental shelf. *Journal of the Geological Society*, **146**, 229–240, https://doi.org/10.1144/gsjgs.146.2.0229.

Texaco 1978. Well 13/3-1 Final Geological Report. Texaco Ireland Ltd., compiled by Stuart, I.A.

Thiyagarajan, S.R., Emadi, H., Hussain, A., Patange, P. and Watson, M. 2022. A comprehensive review of the mechanisms and efficiency of underground hydrogen storage. Journal of Energy Storage, 51, 104490, https://doi.org/10.1016/j.est.2022.104490.

Trueblood, S. 1992. Petroleum geology of the Slyne Trough and adjacent basins. Geological Society Special Publication, 315–326, https://doi.org/10.1144/GSL.SP.1992.062.01.24.

Tyrrell, S., Haughton, P.D.W. and Daly, J.S. 2007. Drainage reorganization during breakup of Pangea revealed by in-situ Pb isotopic analysis of detrital K-feldspar. Geology, 35, 971–974, https://doi.org/10.1130/G4123A.1.

Dinh, V.N., Leahy, P., McKeogh, E., Murphy, J. and Cummins, V. 2021. Development of a viability assessment model for hydrogen production from dedicated offshore wind farms. International Journal of Hydrogen Energy, 46, 24620–24631, https://doi.org/10.1016/j.ijhydene.2020.04.232.

Wall, F., Rollat, A. and Pell, R.S. 2017. Responsible sourcing of critical metals. Elements, 13, 313–318, https://doi.org/10.2138/gselements.13.5.313.

Williams, J.D.O., Gent, C.M.A., Fellgett, M.W. and Gamboa, D. 2018. Impact of in situ stress and fault reactivation on seal integrity in the East Irish Sea Basin, UK. Marine and Petroleum Geology, 92, 685–696, https://doi.org/10.1016/j.marpetgeo.2017.11.030.

Woodcock, N. and Strachan, R. (eds). 2012. *Geological History of Britain and Ireland*, 2nd ed., https://doi.org/10.1002/9781118274064.

Worthington, R.P. and Walsh, J.J. 2011. Structure of Lower Carboniferous basins of NW Ireland, and its implications for structural inheritance and Cenozoic faulting. Journal of Structural Geology, 33, 1285–1299, https://doi.org/10.1016/j.jsg.2011.05.001.

Xiao, Z., Desmond, C., Stafford, P., and Li, Z. 2022. Geological perspectives of offshore underground hydrogen storage in Ireland, EGU General Assembly 2022, Vienna, Austria, 23–27 May 2022, EGU22-1645, https://doi.org/10.5194/egusphere-egu22-1645.

Yekta, A.E., Manceau, J.C., Gaboreau, S., Pichavant, M. and Audigane, P. 2018. Determination of Hydrogen–Water Relative Permeability and Capillary Pressure in Sandstone: Application to Underground Hydrogen Injection in Sedimentary Formations. Transport in Porous Media, 122, 333–356, https://doi.org/10.1007/s11242-018-1004-7.

Ziegler, P.A. 1992. North Sea rift system. *Geodynamics of Rifting*, **208**, 55–75, https://doi.org/10.1016/b978-0-444-89912-5.50007-7.